CDF/ANAL/ELECTROWEAK/CDFR/7865
December 6, 2005

Measurement of the Z Production Cross Section

W. David Dagenhart
Brandeis University

Abstract

We measure $\sigma \cdot B(Z/\gamma^* \to \mu\mu)$ for Z/γ^* in the mass range from 66 GeV to 116 GeV using data from the period between August 2002 and August 2004 with an integrated luminosity of 337 pb^{-1}. The result is 261.2 $\pm$ 2.7 $^{+5.8}_{-6.9}$ $\pm$ 15.1 pb. This measurement is made as a part of the Z dσ/dp_T analysis. The result is not intended for publication by itself, because the previously published CDF run 2 total cross section is already systematics limited. It is also intended as a reference to be used by other CDF analyses when performing the common cross check of reproducing the measurement of the total Z cross section.

Contents

1 Introduction

Previously, the CDF collaboration measured the Z production cross section based on the 72 pb^{-1} of data collected between March 2002 and January 2003. For the muon channel, this result is documented in CDF Note 6711 [1] and was published in PRL [2]. A detailed article has recently been submitted to PRD [3]. It was a very successful analysis. Much of what is documented in this note is based on this earlier work.

This measurement is made as a part of the Z dσ/dp_T analysis. The result is not intended for publication by itself, because the previously published CDF run 2 total cross section is already systematics limited. It is an important cross check for the dσ/dp_T measurement. Many of the details of the Z dσ/dp_T measurement are documented here and will not be repeated in future notes related to that measurement.

Some of the systematic errors and backgrounds currently shown in this note were taken directly from the 72 pb^{-1} analysis. To be specific, these errors are related to the PDF's, the generation of the Z production process in the simulation, and the momentum resolution and scale. The background estimates for the diboson and top backgrounds are also taken directly from the 72 pb^{-1} analysis. This should be adequate for a total cross section measurement, because there is no reason to believe these uncertainties have changed significantly. However, some of these items will be recalculated in the future to complete the Z dσ/dp_T measurement.

Many current analyses study a final state that includes a Z boson or related object. A common cross check for these analyses is to calculate the Z cross section and compare to a previous result. Two and a half years have passed since the 72 pb^{-1} data set was collected. We now have nearly 5 times more data, new reconstruction software, and improved analysis methods. This makes it difficult to compare to the 72 pb^{-1} result and account for all the differences since that time. The electroweak and exotics physics groups have requested a new value for the Z production cross section, which is calculated using a more recent dataset and version of the reconstruction software. This new result will make it easier for other analyses to compare when performing this cross check.

In the sections that follow, we discuss the details of the cross section calculation. Appendix A has further details on direct comparisons of this result to the 72 pb^{-1} result and shows the effect of each change in a step by step order.

2 Dataset and Trigger Path

The data used for this analysis come from dataset bhmu0d, which is made using Stream B (the Inclusive High p_T Muon Sample). This is a primary dataset produced by offline production using software Release 5.3.1. We use data starting with run 150145 (20 August 2002) and ending with run 186598 (22 August 2004).

We select events from the MUON_CMUP18 and MUON_CMX18 trigger paths. The requirements for MUON_CMUP18 are:

- **Level 1** L1_CMUP6_PT4 requires hits on both wires of a CMU trigger wire pair with times within 124 ns of each other. The hits must match an XFT track with $p_T > 4$ GeV/c and a matching pattern of projective hits in 3 out of 4 CMP layers.
- **Level 2**
  - L2_AUTO_L1_CMUP6_PT4 requires nothing other than the corresponding level 1 trigger. Used in runs 141544 to 152949 (16 Oct 2002).
  - L2_TRK8_L1_CMUP6_PT4 requires one XFT track with $p_T > 8$ GeV. This track does not need to be linked to hits in any muon detector. Used in runs 152953 (16 Oct 2002) to 181801 (17 April 2004).
  - L2_CMUP6_PT8 requires an XFT track with $p_T > 8$ GeV linked to hits in the CMU and CMP. Used in run 181839 (17 April 2004) and all later runs.
- **Level 3** L3_MUON_CMUP18 requires a reconstructed muon with a track that has $p_T > 18$ GeV. The muon must be linked to a CMU stub with $|\mathrm{dX}| < 10$ cm and a CMP stub with $|\mathrm{dX}| < 20$ cm (dX is defined as the distance between the extrapolated track and muon stub in the r-ϕ plane).

The requirements for the MUON_CMX18 path are:

- **Level 1**
  - L1_CMX6_PT8 requires hits on both wires of a CMX trigger wire pair with times within 124 ns of each other. The hits must match an XFT track with $p_T > 8$ GeV/c. Used in runs 141544 to 152949 (16 Oct 2002).
  - L1_CMX6_PT8_CSX has the same requirements as the trigger above plus the additional requirement of a CSX scintillator hit in 1 out of the 2 layers. It was used in run 152953 (16 October 2002) and all subsequent runs.
- **Level 2**
  - L2_AUTO_L1_CMX6_PT8 and L2_AUTO_L1_CMX6_PT8_CSX require nothing other than the corresponding level 1 trigger. These were used from run 141544 to 181801 (17 April 2004).
  - L2_CMX6_PT10 requires a 10 GeV XFT track linked to hits in the CMX detector. Used in run 181839 (17 April 2004) and all later runs.

- **Level 3** L3_MUON_CMX18 requires a reconstructed muon with a track with $p_T > 18$ GeV. The muon must be linked to a CMX stub with |dX| < 10 cm.

The XFT requires 4 COT superlayers for the tracks used in these muon triggers. Originally, the XFT required at least 10 hits per superlayer (2-miss). Starting with run 152636 (9 Oct 2002), the requirement was increased to 11 hits per superlayer (1-miss).

3 Good Run Requirements

All runs used in this analysis are required to pass data quality requirements. We use the version 7.0 lists created by the CDF Data Quality Monitoring (DQM) group available here:

http://www-cdf.fnal.gov/internal/dqm/goodrun/v7/goodv7.html

We use the lists that require the following be declared good online: Control, ShiftCr, CLC, L1, L2, L3, COT, and CAL. We also require CAL and COT to be declared good offline. We also require both online and offline declare the CMU, CMP, and CMX to be good. We do not require electron or silicon to be declared good. Run 164844 was removed from the good run list as recommended by the DQM group for stream B. On the DQM web page, this list is labeled as follows: "List for Top/EWK/Exotics" and "muon no silicon".

Good Run List	Integrated Luminosity (pb^{-1})
CMUP and CMX Good	337 $\pm$ 20
CMUP Good	376 $\pm$ 22
CMX Good	342 $\pm$ 20
CMUP Good, CMX Bad	38.4 $\pm$ 2.2
CMX Good, CMUP Bad	5.03 $\pm$ 0.29
Total = CMUP or CMX Good	381 $\pm$ 22

Table 1: Integrated luminosity in dataset bhmu0d in runs with different muon data quality requirements (DQM 7.0 good runs without silicon or electron requirements, see Section 3). This includes data through the August 2004 shutdown.

4 Luminosity

The luminosity is calculated from the run section records in the data following the prescription given here:

http://www-cdf.fnal.gov/~konigsb/lum_official_page.html

The entire bhmu0d dataset was processed using the DHInput module to create luminosity log files. These files include a list of all the run sections in the dataset. A script was written to merge the luminosity log files into one file and remove runs not on a good run list. After running this script once for each different good run list, we had a single new luminosity log file for each good run list. This script was reposited into CVS as Electroweak/scripts/mergeLuminosityLogs.cc. The standard **lumsum.pl** script was used to get the offline luminosities from the database for all the remaining run sections and sum them. The resulting value was multiplied by 1.019, a factor which is related to the extrapolation of the inelastic cross section from $\sqrt{s} = 1.8$ TeV to $\sqrt{s} = 1.96$ TeV [4]. The uncertainty on this luminosity is 5.8%, 4.2% from the CLC luminosity measurement and another 4.0% from the inelastic $p\overline{p}$ cross section [4]. The results of this calculation are shown in Table 1.

As a cross check we compare to the luminosity calculated using a different method by someone else. If the database is queried for the offline integrated luminosity by run instead of by run section, one gets a slightly different result. For the good run list where CMU, CMP, and CMX are all required to be good, the result is 338.2 pb^{-1} [5]. This can be compared to 337.3 pb^{-1} obtained by the method described above. The difference is 0.3%, which is negligible compared to the 5.8% uncertainty. The discrepancy is probably due to the known problem that a small number of data files were lost during production due to repeated crashes of the executable. We assume this is not accounted for in the database in the luminosities by run, but would be properly accounted when the luminosity is summed by run section. If that is the case, 337.3 pb^{-1} is the more accurate result.

There was some concern about a bug that caused empty run sections to be lost during offline production. This would bias the cross section by preferentially dropping some fraction of run sections without Z bosons from the luminosity calculation. We studied this and find it to be a negligible effect for the bhmu0d dataset. The top row of Table 2 shows the number of run sections in bhmu0d and the corresponding luminosity. There are roughly 6 million events in the dataset and since there are about 600,000 run sections we expect about 10 events per

	Number of Sections	Number of Sections with Luminosity > 0	Integrated Luminosity (pb^{-1})	Luminosity Fraction (%)
bhmu0d	636,776	636,752	376	100%
gap size = 1	431	194	0.051	0.01%
1 < gap size < 10	2759	265	0.055	0.02%
gap size >= 10	5245	1688	0.830	0.25%

Table 2: Study of run sections missing from the sequences of run sections in bhmu0d in runs on the CMUP no silicon good run list.

run section. From this alone one would expect there to be few empty run sections. Normally run sections come in sequential order, each section number one higher than the previous section. The bottom three rows show the number of run sections in the gaps in this sequence in bhmu0d. We expect the gaps to usually be 1 section long for cases where Poisson variation caused the run section to be empty. The second row of the table shows this. The associated luminosity is only 0.01% of the total, which is negligible and can be ignored.

We assume the other run sections in the gaps were lost due to operational problems uncorrelated with Z production and therefore we can just ignore these problems.

Note one shortcoming of looking at run section gaps is that you miss the run sections that were lost at the end of runs. This causes the estimates to be a little low. Looking at the last row of Table 2, one can see that 0.25% of the luminosity is lost in the larger gaps. Many of these are probably from the files lost in production. Considering that this estimate fails to include run sections lost at the end of runs, this is consistent the other cross check discussed above.

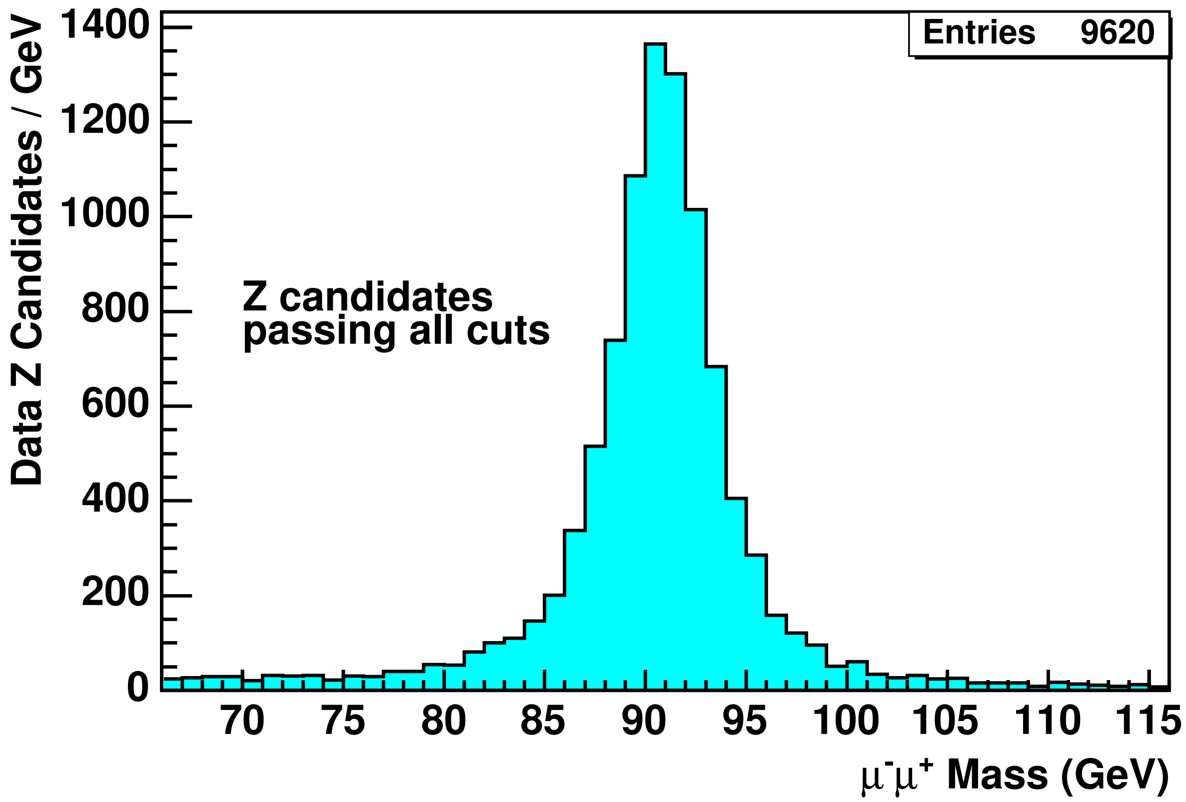

Figure 1: Z candidate mass distribution after all selection requirements.

5 Z Candidate Selection

The complete list of selection requirements for Z boson candidates is shown in Tables 3, 4, and 5. Figure 1 shows the mass distribution of the Z candidates passing all the selection requirements.

5.1 Selection Variable Details

We start with data reconstructed with offline Release 5.3.1, which were created with the latest calibration constants for all relevant quantities. Ntuples were made using Release 5.3.3_nt. We select both legs from **defTracks** and attempt to match them to muons from **defMuons** using the **bestTrack** from the **CdfMuon**. If the tracks are not COT only tracks, we look for a COT only parent of the track. The tracks are then beam constrained and "Larry Corrected" [6].

COT only track or has a COT only parent
Successfully passes beam constrained refit
Not an IO or silicon only track
$p_T > 20$ GeV/c
Not a cosmic
$\rho_{COT} > 140$ cm
COT $\lvert d_0 \rvert < 0.4$ cm
$E_{EM} < 2 + \max(0, (p - 100) \cdot 0.0115)$ GeV
$E_{HAD} < 6 + \max(0, (p - 100) \cdot 0.028)$ GeV
Isolation / $p_T < 0.1$
3 axial segments with at least 5 COT hits
2 stereo segments with at least 5 COT hits
COT $\chi^2/ndf < 4$

Table 3: Selection requirements for both legs of the Z candidate.

Linked to CMU and CMP stubs
Matches TCMD CMUP trigger
CMU $\lvert dx \rvert < 7$ cm
CMP $\lvert dx \rvert < 5$ cm
CMU X-fiducial distance < 2 cm
CMU Z-fiducial distance < -2 cm
CMP X-fiducial distance < 5 cm
CMP Z-fiducial distance < -3 cm
CMP Bluebeam veto for run < 154449
OR
Linked to CMX stub
Matches TCMD CMX trigger
CMX $\lvert dx \rvert < 6$ cm
CMX X-fiducial distance < 6 cm
CMX Z-fiducial distance < -3 cm
CMX Miniskirt/Keystone Veto

Table 4: Additional selection requirements for the trigger leg. At least one leg must pass these additional cuts.

On the "muon nosi" good run list (both CMUP and CMX good)
$\lvert z_0 \rvert < 60$ cm
$\lvert \Delta z_0 \rvert < 4$ cm
Z mass 66 to 116 GeV
Opposite charge

Table 5: Other requirements on the Z candidates.

We use the beam constrained and Larry corrected track whenever possible. To be explicit, these are used for the p_T cut, p used in the E_{EM} and E_{HAD} sliding cuts, p_T in the isolation fraction cut, and also to calculate the Z boson p_T and mass. The beam constrained (but not Larry corrected) tracks are used for the z_0 cuts, the ρ cut, and the muon fiducial cuts. COT tracks that are not beam constrained are used for the cosmic cuts, the track χ^2 cut, and the d0 cut, although d0 is corrected for the position of the beamline. Muon dx, the calorimeter energies, and the isolation energies are calculated using the track from **defTracks**, this is because they are usually obtained directly from the **CdfMuon** object. Even when they are not, we derive them the same way for consistency. From what we have seen, this appears to be the standard way to calculate all of these variables.

Some details on how some of the nonobvious selection variables are calculated.

- ρ_{COT} is the radius of the track at the point where it crosses the Z planes at the ends of the COT.

$$\rho_{COT} = \frac{z_{COT} - z_0}{\lambda}$$

  where z_0 is the track z coordinate at the point of its closest approach to the z axis, λ = cotθ, z_{COT} = 155 cm if $\lambda > 0$, and z_{COT} = -155 cm if $\lambda < 0$. Requiring $\rho_{COT} > 140$ cm is approximately equivalent to requiring the track pass through all 8 superlayers of the COT. For the trigger leg this is necessary because the XFT requires 4 axial layers for the MUON_CMUP18 and MUON_CMX18 trigger paths. For the other leg, one might consider loosening that requirement although it would bring in added complications when calculating the efficiencies and these tracks would have worse momentum resolution.

- The isolation fraction is the calorimeter energy in a cone of radius 0.4 around the track divided by the p_T of the track. This energy is **coneR4Et()** from the **CdfMuon**. p_T is from the track after the beam constraint and "Larry Correction."

- The track χ^2 cut is based on the COT parent track and it is assumed the number of degrees of freedom is 5 less than the number of COT hits.

$$\chi^2/ndf = \frac{\textbf{chi2CT()}}{\textbf{numCTHits() - 5}}$$

- The trigger cuts require a level 1 muon trigger that matches one leg of the Z candidate and a level 3 trigger in the same detector as the muon stub. This determined using the class **MuonTriggerTool** in the MuonUser package, which extracts information from the TCMD bank.

- The muon fiducial distances are calculated using the class **MuonFiducialTool** in the Muon package which is described in CDF Note 5870 [8]. The CMX Miniskirt and Keystone were explicitly set dead and the CMP Bluebeam was set dead for runs less than 154449 when using the **MuonFiducialTool**.

5.2 Differences in Selection Requirements

Careful review of the run 2 analyses using high p_T muons shows that there is not a standard set of muon selection requirements used by all analyses. There are small variations from one analysis to the next, although the requirements are always very similar. In the list below, we discuss the differences between our selections and those documented in CDF Note 7367 [7].

- We loosen the CMU dX cut from 3 cm to 7 cm, because the simulation does not model this distribution well. There are significant tails in the data distribution in this range that are negligible in the simulation. The efficiency for a muon to pass the CMU dX cut increases by 4% and the overall number of Z candidates increases by about 1%. One might worry that this would increase QCD background, but loosening this cut does not allow any same sign candidates into the sample of Z candidates.

- For the z_0 cut, we use the average z_0 of the 2 legs as our estimate of the event primary vertex z0 rather than making the requirement on the z_0 of both legs. Cutting on both legs effectively makes the estimate of the event vertex to be the minimum z_0 of the two legs, which is slightly biased low.

- The cosmic cut is made by directly running the dicosmic fit [9] on the legs of the Z boson candidate instead of using the CosmicFinderModule to select the tracks. Otherwise, the requirements are the same as in the CosmicFinderModule. If for either track the dicosmic fit returns 0 or 1, the χ^2 of the dicosmic fit is less than 1000, and the track is consistent with downgoing, then the candidate is tagged as a cosmic. We make the additional requirement that the 3 dimensional angle between the Z legs be greater than 2.8 radians for a candidate to be removed from the Z candidate sample. The few candidates tagged as cosmic with smaller angles have characteristics similar to Z candidates not cosmics. The angle restriction adds 8 candidates to our final Z sample. On close examination of these 8 candidates, it appears the dicosmic fit picks up hits unrelated to either Z leg that randomly happen to be opposite one of the legs. A final comment here, if cosmics were appearing in the final sample without both cosmic legs corresponding to both Z legs, half of them would show up as same sign events in the final sample. There are none. Therefore, the angle must be close to π for cosmics. The results of this cosmic identication procedure are nearly identical to the CosmicFinderModule results. We like this change mostly because it is easier to describe exactly what we are doing to someone not familiar with the CosmicFinderModule. In the rare cases where there are differences, it is also the more correct thing to do.

- We do not cut on the silicon impact parameter, even when it is available. There are 19 candidates in the final sample that would fail a silicon impact parameter cut. We examined several of them and found that they were more consistent with problems in silicon reconstruction than with being high impact parameter tracks. They look like good Z boson candidates. We do not care about silicon reconstruction problems and decided to not remove these candidates. This simplifies the analysis by reducing our dependence on the silicon.

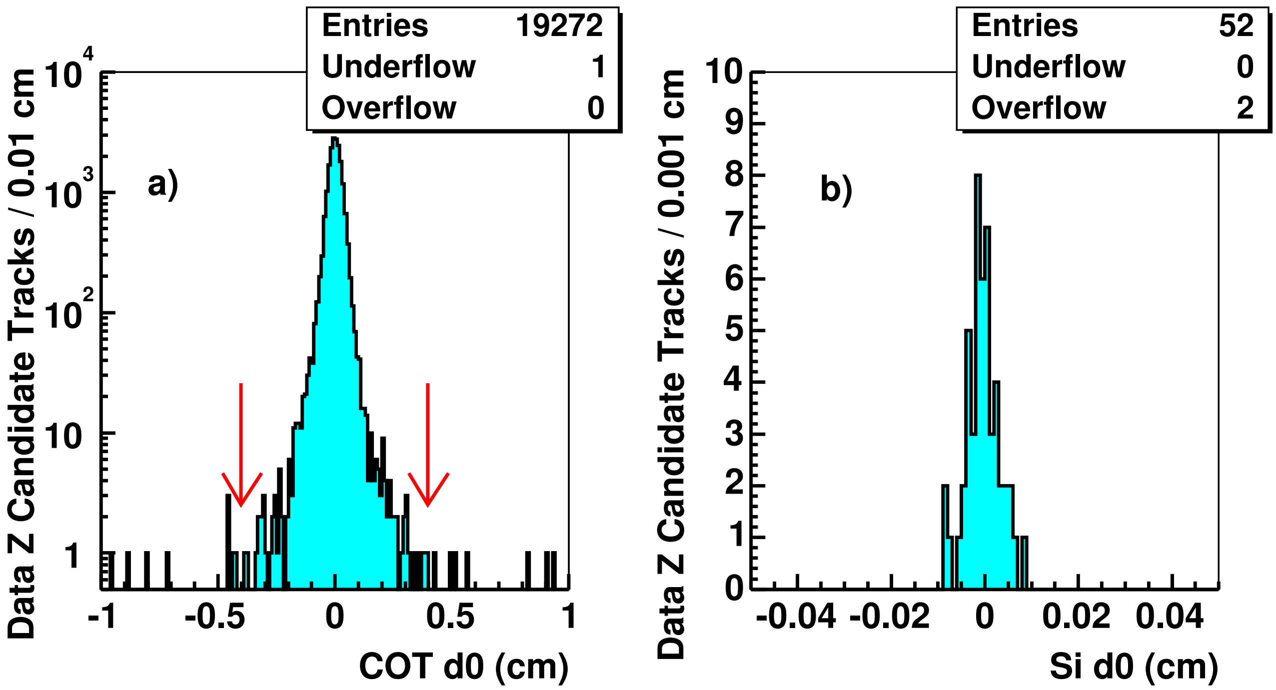

Figure 2: Impact parameter distributions for Z candidates passing all cuts except the impact parameter cut. (a) COT impact parameter distribution. (b) Silicon impact parameter for tracks with COT impact parameter between 0.2 cm and 0.4 cm.

- We require the COT impact parameter to be less than 0.4 cm instead of 0.2 cm. An impact parameter 0.2 cm is still in the central part of the distribution. By examining the silicon impact parameter of these candidates added by loosening this cut, one can see that they are not high impact parameter events. See Figure 2.

- We add CMU fiducial requirements for the trigger leg, because in principle one should use the same fiducial cuts in the analysis as are used to calculate the muon reconstruction efficiencies and scale factor. One has to use some CMU fiducial cuts to calculate the muon reconstruction efficiency, so there needs to be a cut. We widen the fiducial cuts in the x direction for CMP and CMX from 0 cm to 5 cm and 6 cm respectively. The muons in this range are perfectly fine and can pass the standard dx cuts.

These selections were developed for a measurement of the p_T distribution of Z boson production. In this measurement, the backgrounds are negligible and we want to avoid geometric regions with poor momentum resolution or where the efficiencies are not well understood. If one were performing a search, one might consider loosening the muon fiducial cut in the Z direction or loosening the ρ_{COT} cut for the second leg to increase the acceptance. If one were looking for muons that were not legs of Z bosons, one might consider making some cuts tighter to decrease backgrounds.

5.3 Additional Selection only for Simulation

This section describes a cut that affects so few Z candidates that one could safely neglect the whole issue. But in principle, it is correct to make this cut. It is also a nice cross check to look for Z candidates coming from this source.

It is possible to have a Z candidate in an event with a real Z boson, where one of the reconstructed legs comes from a particle other than one of the muons from the Z decay. These candidates should show up with roughly the same number of same sign and opposite sign candidates. These are accounted for in our same sign background estimates. There are no same sign data candidates so we know there are very few candidates like this in data.

Unlike other backgrounds, these will also show up in the simulation and if they are not explicitly removed, they get accounted for in the acceptance. Essentially, this corrects for the effect twice (once in the acceptance and once as a same sign background). So we look for them and remove them.

In simulation one can remove this category of candidates by requiring that the HEPG muons from Z decay match the reconstructed legs of the Z candidate. We make the very loose requirement that ϕ of the HEPG momentum matches ϕ of the reconstructed track within 0.02 radians.

We have 168,043 Z candidates passing all selections in our simulation sample. We find 4 Z candidates where the HEPG and reconstructed legs fail to match. There are another 3 candidates where both legs have the same sign of charge that fail to match. We examined these 7 candidates to see why the leg that does not match passed the calorimeter cuts. In 5 of the 7 cases, the track crossed z = 0 before reaching the CMU and likely hit the calorimeter crack. In one case, the leg was a muon from charm decay. In the other case, the leg was from a K short that decayed in the COT and the corresponding reconstructed track had the momentum direction so poorly measured that it did not point to the correct calorimeter towers.

In 2 of the 7 cases where there the match failed, there was another Z candidate in the same event which passed the matching cut and all the other cuts. We checked all the data and simulation, and found that in every event there was 0 or 1 candidate passing all cuts. We could find no events with 2 or more Z candidates passing all cuts.

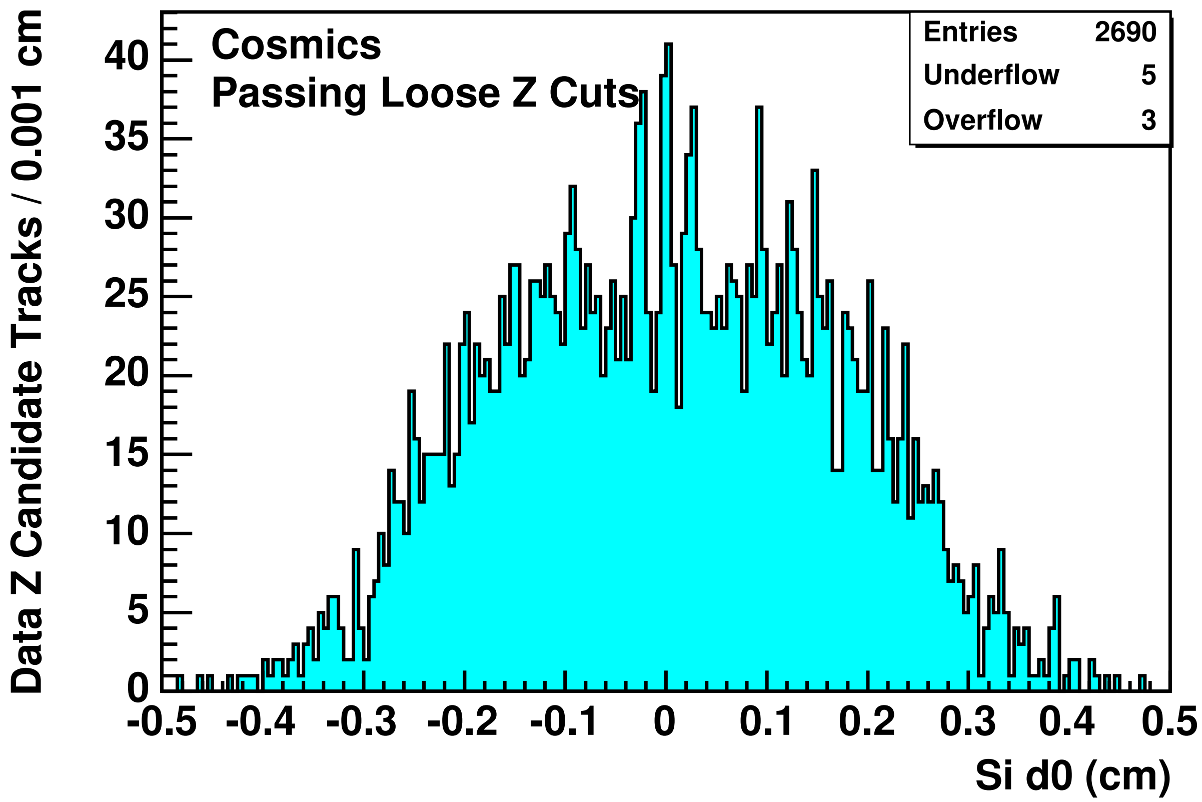

Figure 3: Silicon impact parameter for legs of candidates tagged as cosmics and passing loose Z cuts described in the text.

6 Backgrounds

6.1 Same Sign Background

If one modifies the selections to require that the muon legs have the same sign charge instead of the opposite sign charge, then one finds no same sign candidates. Based on this fact, we conclude that the same sign backgrounds are negligible. To be quantitative about it, a Bayes upper limit of about 1.1 events. We neglect this background in the cross section and error calculations.

The same sign backgrounds include candidates where one or both muon legs are associated with hadronic jets. This is also called QCD background. These muons can be real or fake, but in either case they should appear nearly as often with the same charge as with opposite sign charge.

6.2 Cosmic Background

The next 2 sections provide details of our estimate of the number of cosmics in the final Z sample and also an estimate of the number of Z's removed by the cuts that remove the cosmics. In both cases the estimates are consistent with 0 and we derive an upper limit on

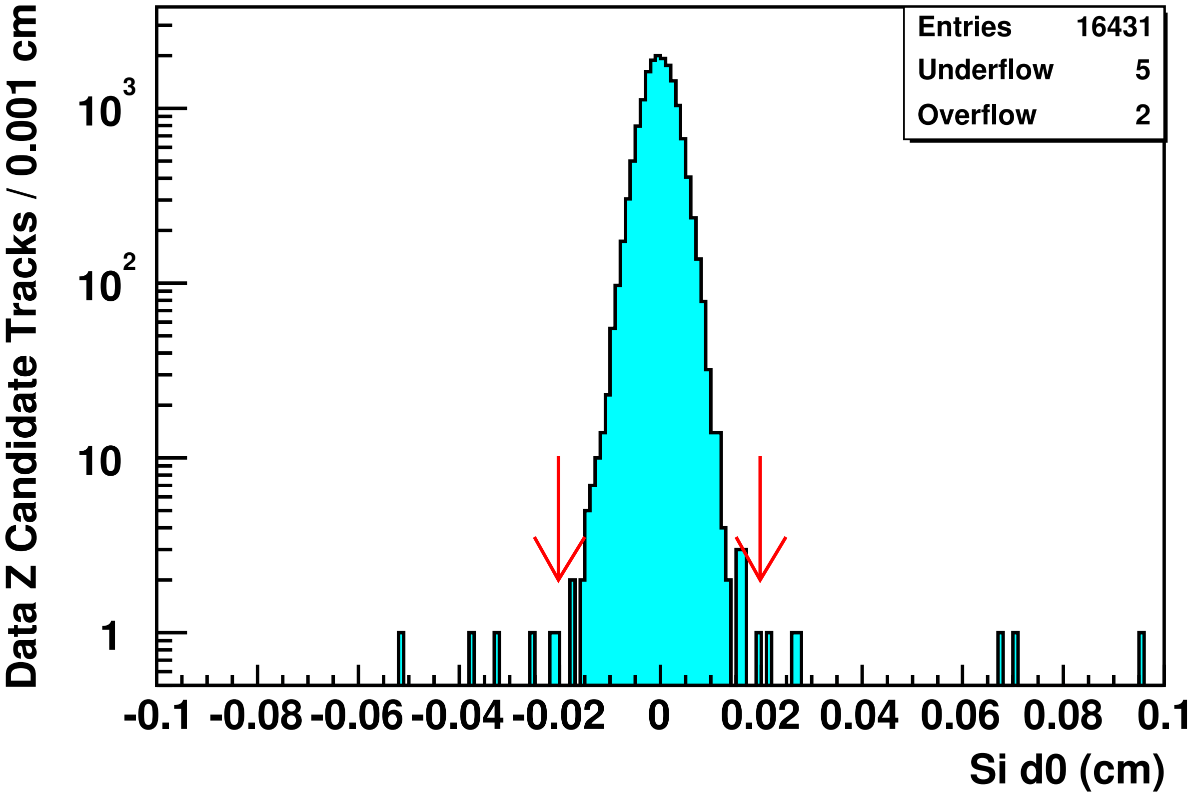

Figure 4: Silicon impact parameter for legs of Z candidates passing all cuts having silicon hits.

the number of them. We estimate less than 6 cosmics survive in the final Z sample. This is 0.06%. We estimate less than 3 Z bosons are removed by the cosmic cuts. This is 0.03%. These are negligible amounts compared to other uncertainties in this analysis and the cosmic background is simply ignored in all other calculations.

6.2.1 Cosmics in the Final Z Sample

We use the impact parameter distribution measured in the silicon detector and the dimuon mass distribution to estimate the number of cosmics in the final Z sample. We expect the Z bosons to have a small impact parameter and a mass distribution peaked near 91 GeV. Cosmics will not.

The first step is to work with the subsample of Z candidates which have both legs pointing at good silicon. Here are the requirements we use to select this subsample.

- The event must be in a silicon good run per the DQM 7.0 good run list.
- $|z_0| < 30$ cm where z_0 is the average z_0 of the two legs.
- Require both legs to point at good silicon wedges. The definition of good wedges is motivated by CDF Note 6088 [10]. A wedge is 30 degrees in ϕ with wedge 0 starting

at $\phi = 0$. If $|z_0| < 0$, the bad wedges are 6, 7, and 11. If $|z_0| > 0$, the bad wedges are 6 and 8. If track ϕ is in the range covered by one of these bad wedges, the track does not point at good silicon.

There are certainly better ways one might do this (maybe using **SiExpected**), but this set of criteria is good enough. It is also simple and easy to use.

We need to correct for the fact that we are only looking at a subset of the cosmics by requiring that the legs point at good silicon. To get a correction factor we look at a sample of cosmics and count the number of candidates where both legs randomly point at good silicon. The ratio of all the cosmics to the ones that point at good silicon is the correction factor.

We select a sample of cosmics by requiring two legs that are COT only beam constrained tracks with $p_T > 20$ GeV, $\rho_{COT} > 140$ cm and COT $|d_0| < 0.4$ cm. They also need to be flagged as cosmics by the dicosmic fit. There are 3328 cosmics in this sample and 1591 have both legs pointing at good silicon. The correction factor is 3328 / 1591 = 2.09.

Figure 3 shows the silicon impact parameter distribution of the legs that have silicon hits from candidates in the cosmic sample described above which have both legs pointing at good silicon. Figure 4 shows the same distribution for legs with silicon hits from Z candidates that pass all Z selection requirements. It is clear that the cosmic distribution is much broader and this is a powerful variable for separating cosmics from Z's in our sample.

Next, we select a subsample that contains most of the cosmics that are in the final Z sample. We plot the dimuon mass distribution of Z candidates passing all Z selections, require that both legs point at good silicon, and that neither leg has a silicon impact parameter less than 0.02 cm. This is shown in Figure 5. In all but 1 of these 36 candidates, both tracks have no silicon hits.

We need another correction factor to account for the number cosmics that randomly have one leg with a silicon $|d_0| < 0.02$ cm. In the cosmic sample defined above, 135 of the cosmics have a leg with silicon $|d_0| < 0.02$ cm. The correction factor is the ratio of the number of cosmics with legs pointing to good silicon to the number of them that do not have a leg with $|d_0| < 0.02$ cm. This is 1591 / (1591 - 135) = 1.09.

There are only 36 Z candidates with legs pointing at good silicon that fail to have a leg with a small silicon impact parameter. Further, we can see from the Figure 5 that their mass distribution looks like a Z boson mass distribution not like a cosmic mass distribution. For comparison, Figure 6 shows the mass distribution of the sample of candidates flagged by the dicosmic fit as cosmics and passing loose Z cuts. The distribution looks linear not peaked.

We can estimate the cosmic background in Figure 5 using a sideband technique. Define a central bin between 81 and 101 GeV. The sidebands are outside that region. There is one candidate in the sidebands. The ratio of the full range of the plot to the range of the sidebands is 50 / 30 = 1.67. We can also estimate the number of Z's in the sideband based on the number of candidates in the central bin. If one calculates the ratio of the number of candidates in the sidebands to the central bin using the sample of Z candidates that pass the analysis cuts (Figure 1) one finds the ratio is 760 / 8860 = 0.0858. We should expect 0.0858 x 35 = 3.0 Z bosons in the sidebands in Figure 5. This is clearly consistent with zero cosmics being in the final sample.

We calculate a Bayesian upper limit on the number of cosmics in the Z sample as follows

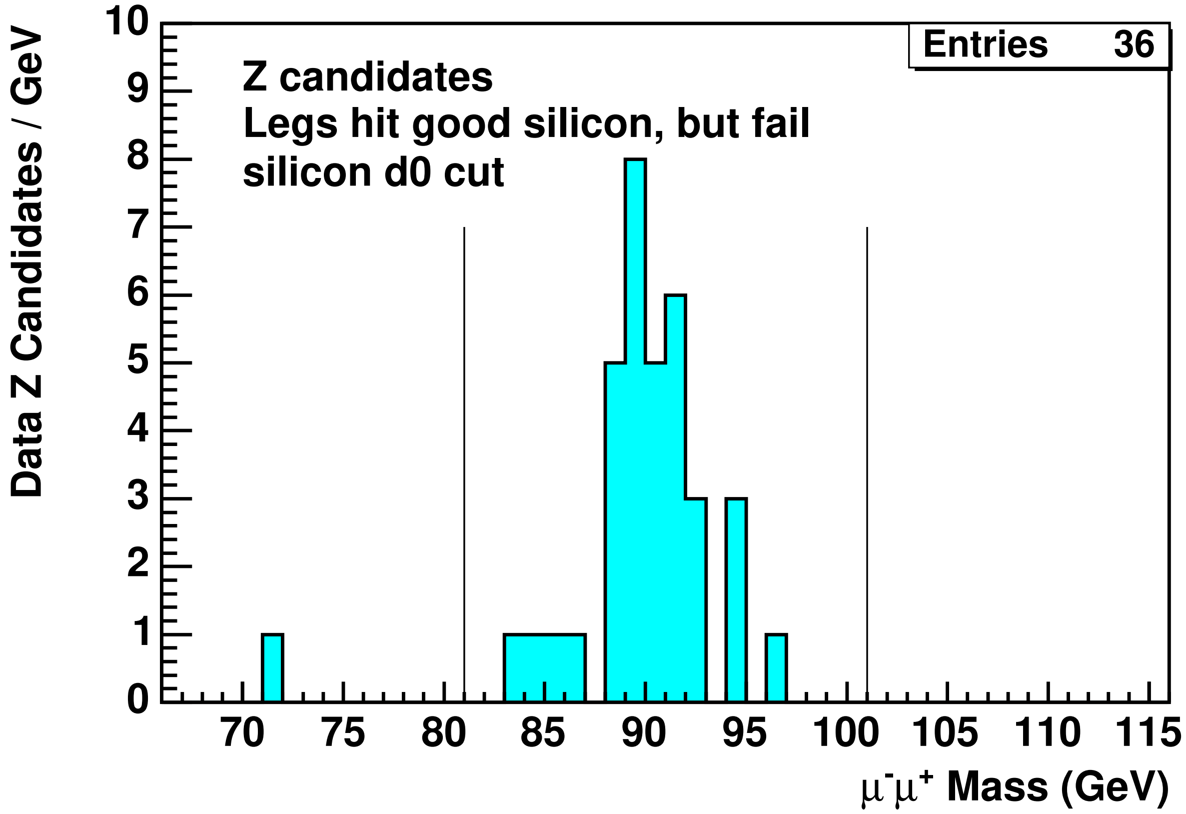

Figure 5: Z candidate mass for candidates with legs pointing at good silicon which fail to have a track with silicon impact parameter less than 0.02 cm. This should include most cosmics surviving in the final Z sample.

(following the prescription in the PDG). We assume a nonnegative, but otherwise flat prior. The number of candidates observed is 1. The expected background is 3.0. The 68% Bayesian upper limit is 1.46. We need to multiply by the scale factors calculated above to account for the cuts we have made. The final upper limit is 1.46 x 2.09 x 1.09 x 1.67 = 6 cosmics in the final Z sample (rounded to 1 significant digit).

Repeating the same procedure for the subsamples used to measure the muon reconstruction efficiencies and the muon ID efficiencies yields very similar answers.

6.2.2 Z Bosons Removed by the Cosmic Cut

We need to estimate how many Z's are removed by the cosmic cuts. The order cuts are made is important when calculating the efficiency that a Z will pass a cut. We calculate the muon ID efficiencies and muon reconstruction efficiencies from data after the cosmic cut has been made, and therefore we need to calculate the number Z's removed by the cosmic cut using a loose sample before any muon ID or muon stub cuts are made. We do the calculation using Z candidates that have passed the following loose cuts: COT only beam constrained tracks with $p_T > 20$ GeV, $\rho_{COT} > 140$ cm, one leg passing the muon fiducial cuts, z_0, Δz_0, Z Mass, and muon charge cuts (see Section 5 for more details on cuts). The dimuon mass

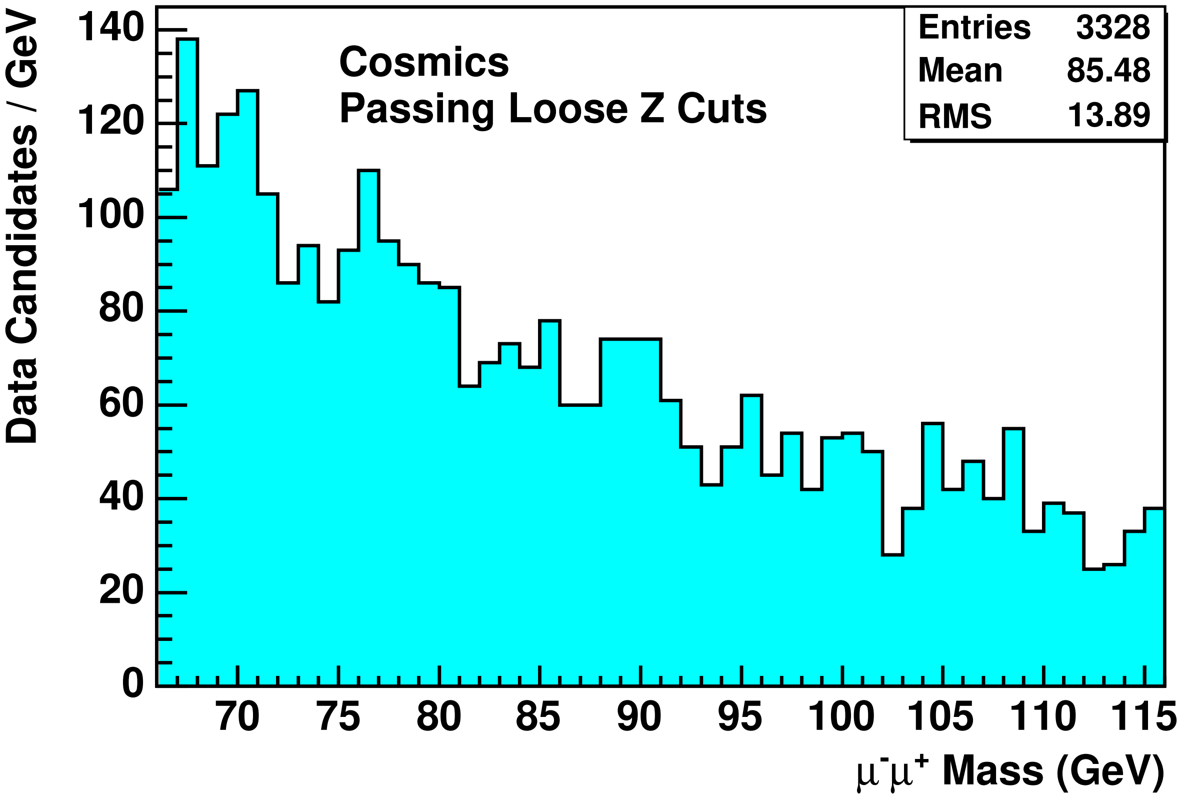

Figure 6: Z candidate mass for candidates passing loose Z cuts, but flagged as a cosmic by the dicosmic fit.

distribution of these candidates is shown in Figure 7.

The following is the procedure to identify and remove cosmics from the Z sample:

- Examine candidates only if the 3 dimensional angle between the Z legs is greater than 2.8 radians.
- Test by running the dicosmic fitter [9] twice, once using each Z leg as a seed.
- Criteria: Dicosmic fit converges with result that is consistent with a downgoing cosmic track with $\chi^2 < 1000$.
- If either leg is flagged by the dicosmic fit as a cosmic the Z candidate is removed.

The dimuon mass distribution of the loose Z candidates that are identified as cosmics is shown in Figure 8. There is no evidence of a Z mass peak in this distribution, but we can get a better estimate of the number of Z's in these events by looking at some other variables.

First, divide the sample into those events where both dicosmic fits flagged the candidate as a cosmic and those where only one dicosmic fit was consistent with a cosmic. Figure 9 shows the direction of the cosmics where both legs were tagged as cosmics. Note that all the entries are downgoing and none are upgoing. Cosmics should almost always be downgoing.

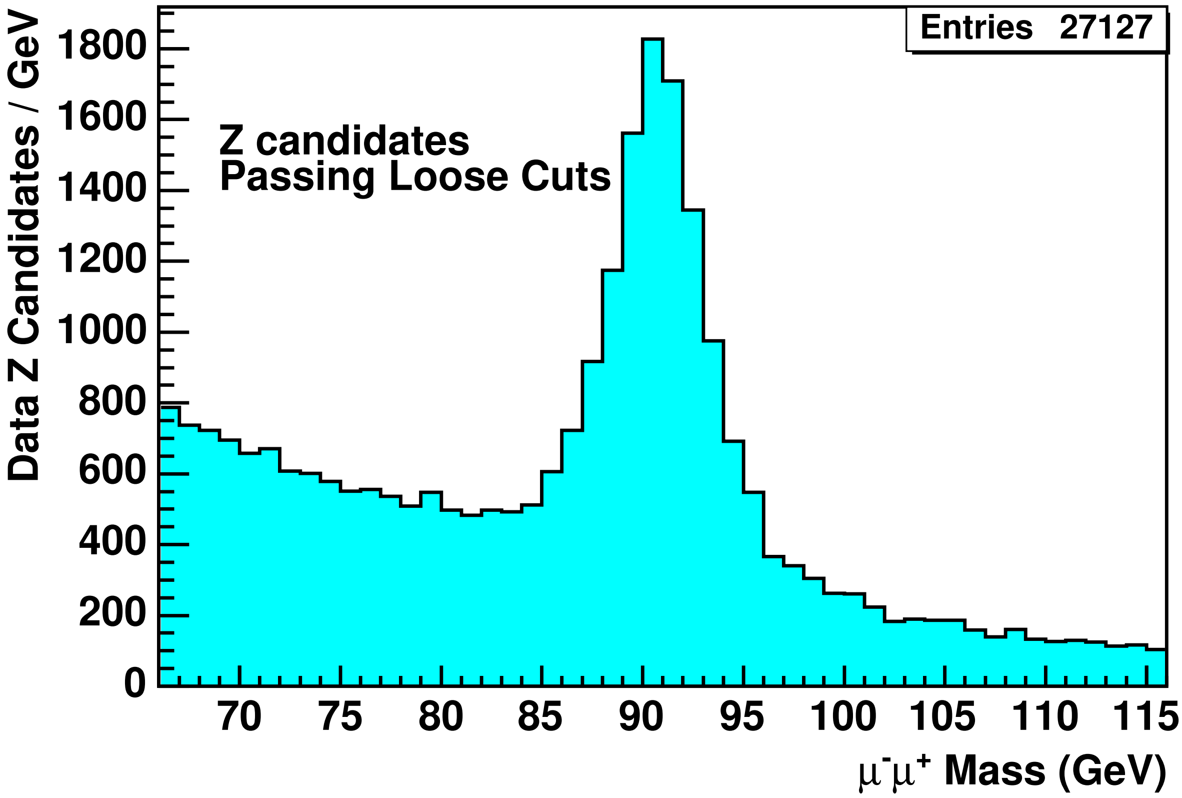

Figure 7: Z candidates passing loose cuts without any muon ID or muon stub cuts.

The only exception would be muons from cosmic neutrinos, but these should be extremely rare. Z's and other kinds of background should be roughly distributed equally between upgoing and downgoing candidates. We conclude there are no Z's removed in the case when both legs are tagged as cosmics.

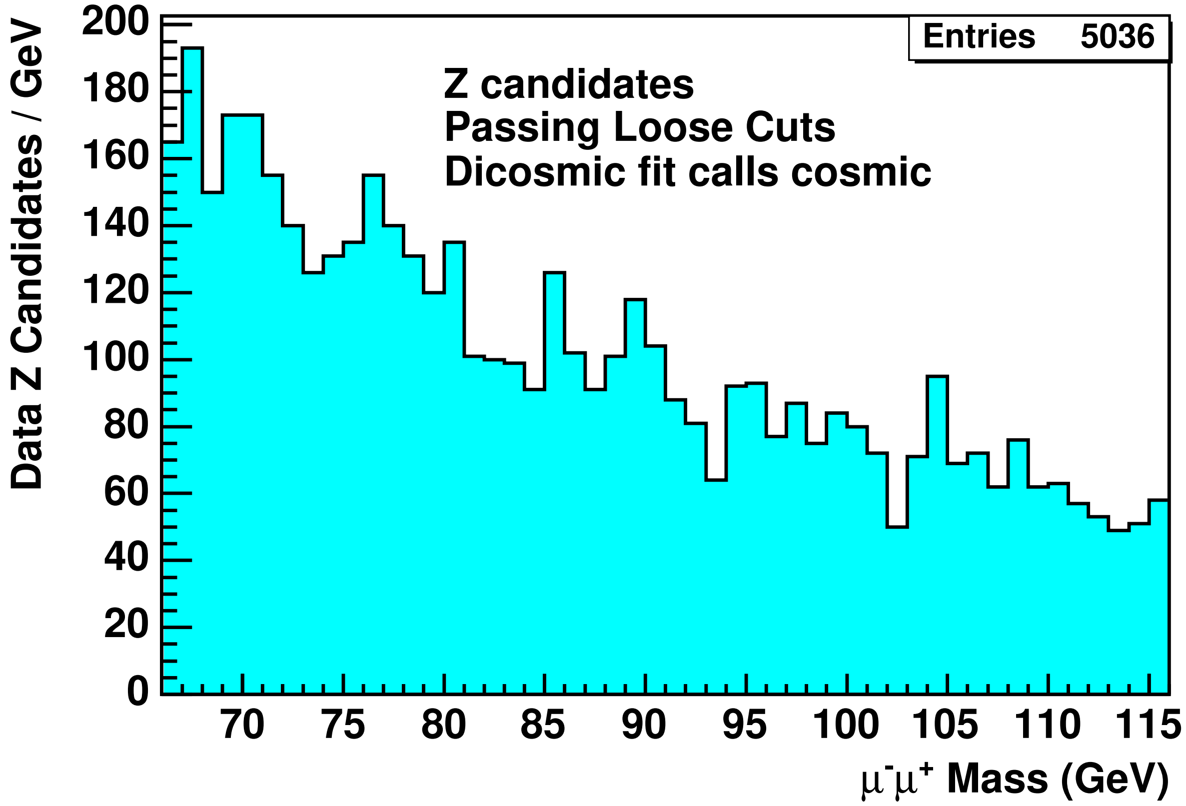

Figure 8: Z candidates passing loose cuts and also flagged as cosmic by the dicosmic fit.

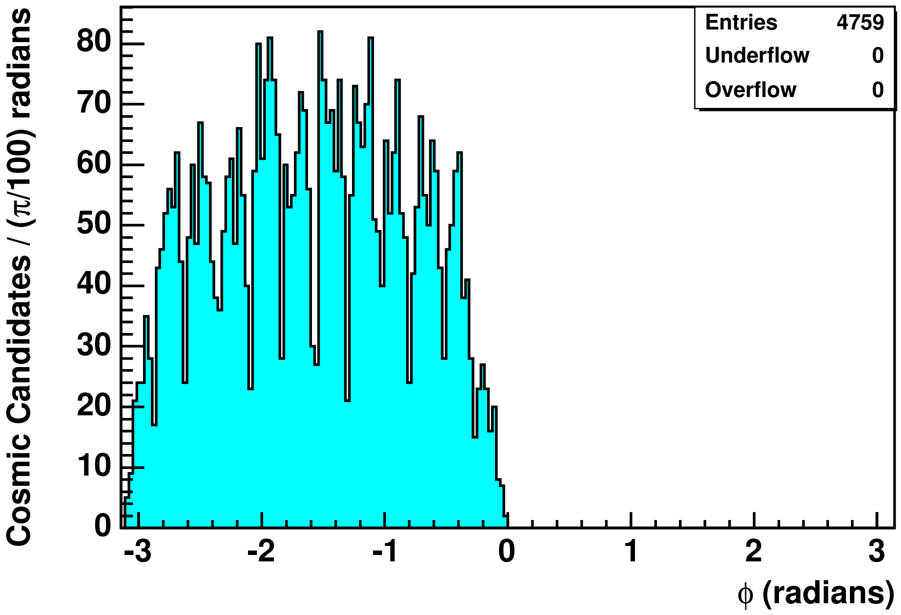

Figure 9: Track ϕ for Z candidates where both dicosmic fits call the candidate a cosmic. Track ϕ of the leg called outgoing by the dicosmic fit is plotted. All these candidates pass the loose Z cuts described in the text.

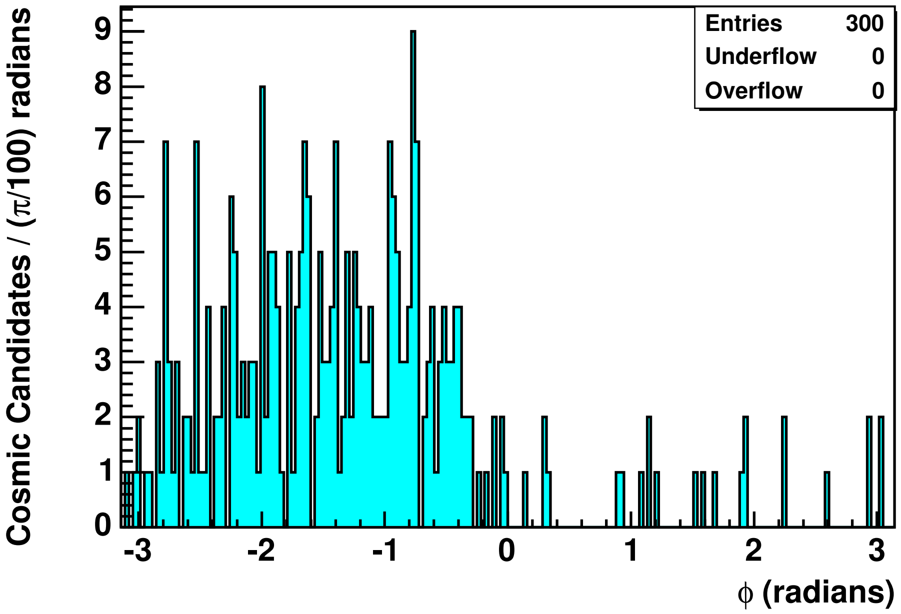

Figure 10: Cosmic ϕ for Z candidates where only one of the dicosmic fits calls the candidate a cosmic. If the seed leg is called outgoing by the dicosmic fit, its ϕ is plotted. If the seed leg is called incoming, ϕ in the opposite direction of the track ϕ is plotted.

Figure 10 shows the ϕ distribution in the other case when only one leg is called a cosmic by the dicosmic fit. Most of these are downgoing as well, and we conclude that most of these are also cosmics. But there are 23 candidates that are upgoing and we assume that roughly the same number of noncosmics exists in the downgoing sample. These may be Z's or QCD background. We study the silicon impact parameter and EM calorimeter energy to differentiate between these possibilities.

We could think of two cases where a Z might be called a cosmic by the dicosmic fit.

- When there are problems with the COT hits on a track that are severe enough for the dicosmic fit to get the direction wrong. We assume that this will usually affect one Z leg but not both. The quality of the two tracks should not be correlated.
- Both Z leg tracks are good, but there are unrelated hits opposite one track that are picked up by the dicosmic fit.

In both these cases, one of the Z legs should have a good track and we can look for it. Start by restricting ourselves to the subsample of events where both legs are pointing to good silicon as defined in the previous section. Figure 11 shows the minimum d_0 of the two Z legs for candidates where only one leg is tagged as cosmic. There are 14 candidates in the peak near zero. Most of these are either QCD background or muons from Z decay. The 4 candidates outside of the peak near zero are likely cosmics which should be randomly spread over the range of that plot. Divide the plot into a central bin between -0.01 cm and 0.01 cm. This includes the central peak of 14 candidates. We expect there will be 4 x (0.01 / 0.09) = 0.44 cosmics in this central bin.

One can separate the QCD background from the Z's by looking at the EM calorimeter energy. One expects that usually at least one of the Z muons will have a small EM energy. Figure 12 shows the EM energy distribution for these candidates. The smaller EM energy of the two legs is plotted. Only the 14 candidates in the central bin between -0.01 and 0.01 in Figure 11 are included in the plot. Note that all but one of these candidates has an EM energy for both legs greater than 2 GeV and only one has a small electromagnetic energy. Except for that one candidate these candidates are consistent with QCD background. This one candidate could be either a Z boson or a cosmic.

We calculate a Bayesian upper limit on the number of Z's removed by the cosmic cuts (following the prescription in the PDG). We assume a nonnegative, but otherwise flat prior. The number of candidates observed is 1. The expected background is 0.44 cosmics. The 68% Bayesian upper limit is 2.03. We need to multiply by a correction factor to account for requiring that both legs point at good silicon. If one looks at the full sample of Z candidates one finds that 6813 out of 9620 have both legs pointing at good silicon. The correction factor is 9620 / 6813 = 1.4. The final upper limit is 2.03 x 1.4 = 3 Z's removed by the cosmics cuts (rounded to 1 significant digit).

As a cross check we show plots similar to Figures 11 and 12, but modify the requirements to require the 2 candidate Z legs have the same sign of charge. Here we expect to see only QCD background. Figure 13 shows the d_0 distribution and the number of events in the central peak is similar to the opposite sign case. The EM energy distribution shows that all the events have large EM energy. This is consistent with our expectation because we expect all the same sign events to be QCD background.

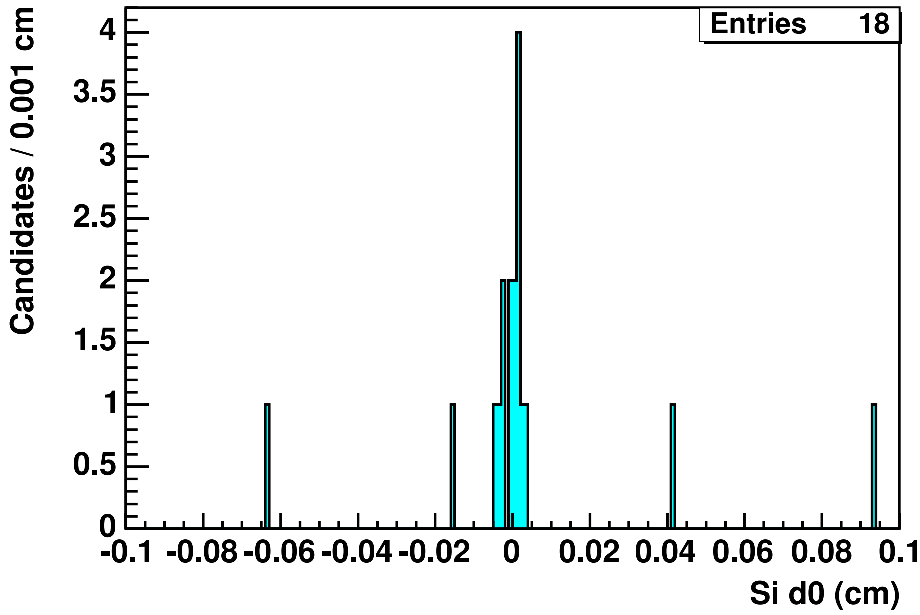

Figure 11: Silicon impact parameter distribution of loose Z candidates with one leg tagged as cosmic and both legs pointing to good silicon. The smaller silicon impact parameter of the 2 Z legs is plotted. Only includes candidates where this exists and is less than 0.1 cm.

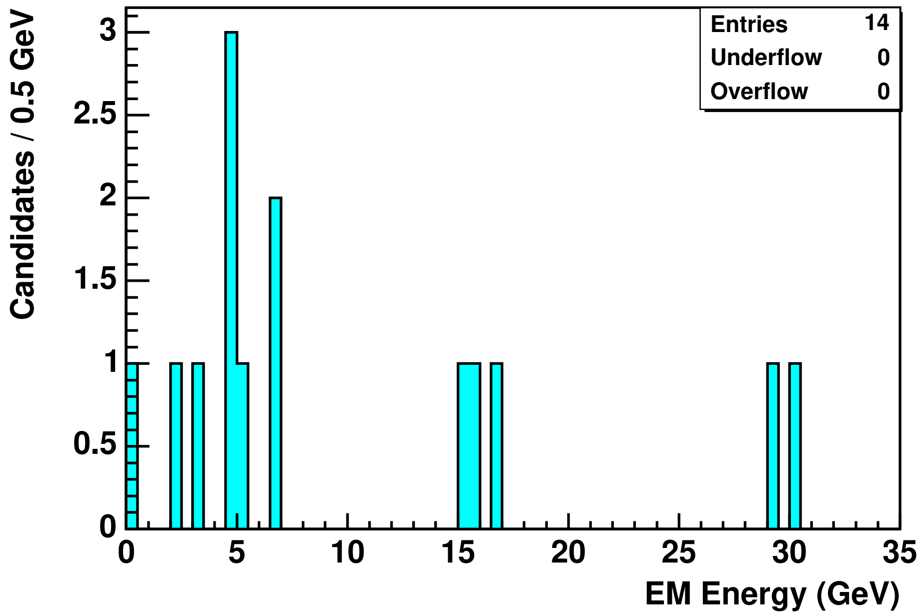

Figure 12: EM calorimeter energy for Z candidates in the central peak of the preceding figure. The smaller EM energy of the two legs is plotted.

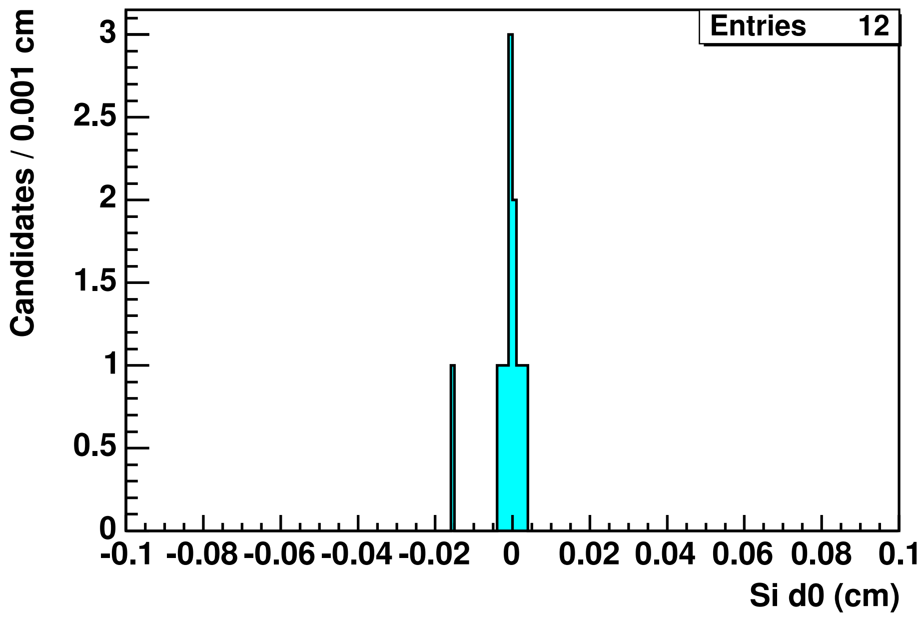

Figure 13: Similar to Figure 11 except the two Z candidates legs have the same sign charge. Silicon impact parameter distribution of candidates tagged as cosmics and passing loose Z cuts, except the charge cut. The smaller impact parameter of the 2 Z legs is plotted. Only includes candidates where this is less than 0.1 cm.

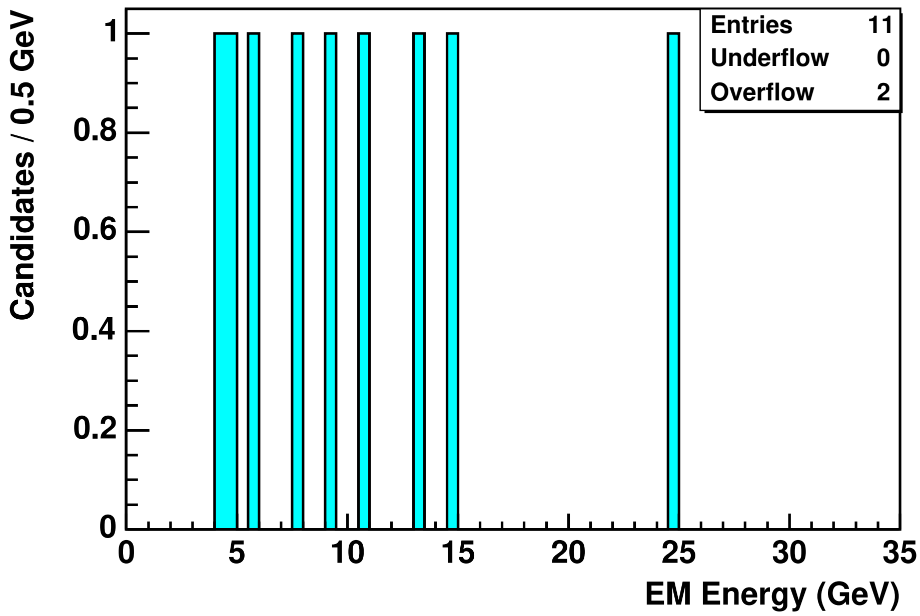

Figure 14: Similar to Figure 12 except the two Z candidates legs have the same sign charge. EM calorimeter energy for Z candidates in the central peak of the preceding figure. The smaller EM energy of the two legs is plotted.

Background	Expected Number of Events	Percentage
Z→ $\tau\tau$	8 ± 2	0.08 ± 0.02 %
Cosmic	< 6	< 0.06 %
WW	< 5	< 0.06 %
WZ	< 5	< 0.06 %
$t\bar{t}$	< 5	< 0.06 %
Same Sign (including QCD)	< 1.1	< 0.01 %

Table 6: Summary of Backgrounds

6.3 Other Backgrounds

Currently, we rely on the estimates from the 72 pb^{-1} analysis for the other backgrounds (see Section VII. D. of the submitted PRD article [3]). These background estimates were based directly on simulation.

The Z→ $\tau\tau$ background was estimated to be 1.5 ± 0.3 background events per 1785 signal events. We simply scale this by a factor of 9620/1785 (the ratio of the Z signal between the new and old analyses). We correct for this in the final result, even though it is a very small correction. The diboson and top backgrounds were estimated to be less than 1 event per 1785 signal events, or less than 0.06%. We neglect these backgrounds when calculating total cross section.

Alternatively, one could look at the WW analysis documented in CDF Note 6909 [11]. Table 45 on page 70 of that note shows that in the $\mu\mu$ channel their expected WW signal is 2.48 ± 0.29. Figure 31 on page 82 of Note 6909 shows the mass distribution of these candidates. Using the figure and a ruler, one can estimate that the fraction of their WW signal with dilepton mass in the range 66 to 116 GeV is roughly 0.38. The ratio of luminosity of this Z cross section analysis to the WW analysis is 337 / 184. Multiplying these values yields 1.7. Table 6 of Note 6909 shows the effect of additional cuts that are not made in this Z cross section analysis that remove roughly 60% of the WW signal. Taking this into account, we would expect about 3 WW events in our Z sample. There are large uncertainties in this estimate and smaller factors that we have not accounted for, but it is clear from the magnitude of the result we are safe in neglecting this background. This estimate is also consistent with the value in Table 6.

6.4 Background Summary

Table 6 summarizes the backgrounds.

7 Acceptance

We use simulation dataset zewk6m to calculate the acceptance. (Thanks to Kathy Copic who did the work to generate this dataset). This simulation dataset is generated with Pythia version 6.216 [12] using the following settings:

- The center of mass energy is set to 1960.
- MSEL is set to 11 for Z/γ^* production with a minimum $\sqrt{\hat{s}}$ of 20 GeV (CKIN(1)).
- The Z/γ^* is required to decay to $\mu\mu$.
- The CTEQ5L parton distribution functions are used.
- We use the Willis Sakumoto tune for Z p_T, which is based on the run I measurement.
  - MSTP(91) is set to 1 for a gaussian distribution of the primordial $k_\perp$ distribution in the hadron with width, PARP(91), set to 2.10 and upper cutoff, PARP(93), set to 15.0.
  - PARP(62) is set to 1.25. This is the effective cutoff Q or $k_\perp$ below which space-like parton showers are not evolved.
  - PARP(64) is set to 0.2. In space-like parton shower evolution, the squared transverse momentum evolution scale $k_\perp^2$ is multiplied by PARP(64) for use as a scale in α_s and parton distributions.
- We use Tune A from Rick Field to better simulate the underlying event.
- We use the run dependent scheme to approximate the variation in instantaneous luminosity. We use run list v7_1001. (See Dave Waters talk in the Electroweak group on 2 September 2004.)

There are 3,257,840 events in zewk6m. We only use simulated runs that are on the same good run list used to select real data. In addition, we also remove simulation events from runs 150990, 151092, 151116, 151121, 151140, 151141, 151142, 151228, 151229, 151231, 151237, 154050, 154054, 154069, 154070, 154710, 154768, 154799, 154829, 154841, 154856, 154860, 154861, 155155, 168125, 175596, 176576, 176584, 176631, 176632, 176633, 177140, 178254, and 182890. There is a problem with primary vertex in these simulation runs that does not exist in data. This is associated with a bug that affected this simulation dataset. See the presentation by Michael Schmitt at the Joint Physics Meeting on 25 March, 2005.

In addition, we found that 2 of the files in zewk6m could not be read to the end without the executable crashing. So we processed only the first 5000 events in zm029012.0002ewk6 and the first 4000 events in zm02d3a0.0002ewk6. We skipped the 2024 events at the end of those files.

After generation, the standard **CdfSim** detector simulation is run and then the simulated events are reconstructed. For these processes we use software release 5.3.3 plus the "Electroweak Patches". The patches modify the simulated COT hit resolutions to make them more like data. This shows up primarily in the COT track χ^2 and Z mass distributions.

The acceptance is calculated by taking the ratio of

$$\frac{\text{Reconstructed Z Bosons}}{\text{Generated Z Bosons}}$$

When counting generated Z bosons, we count all Z bosons in HEPG that pass the following requirements (each Z boson appears twice in HEPG, but gets counted as 1 Z boson).

- Passes the good run requirements.
- The z coordinate of the Z boson production vertex is within 60 cm of z = 0. This is based on the OBSV vertex position (which is selected based on the links from the negative HEPG Z decay muon to the corresponding OBSP particle and then to the corresponding OBSV vertex).
- The mass of the Z boson lies between 66 GeV and 116 GeV. This is based on the momentum from HEPG using the momentum before final state radiation (which can be taken from the Z boson in HEPG or first pair of decay muons in HEPG).

We count reconstructed Z bosons that pass the same selection requirements as the data Z candidates with the following two exceptions.

- No trigger selection is made on the simulated events. We do not use the trigger simulation.
- We add the requirement that the reconstructed Z boson match the generated Z boson in HEPG (see Section 5.3).

Except for the trigger efficiency, we use all the other cuts including ones where the efficiency is calculated from data. In those cases, the scale factor described later is used to account for differences between data and simulation efficiencies.

The acceptance is 168,043 / 1,376,349 = 0.12209 ± 0.00028.

7.1 Data Simulation Comparison Plots

On the next several pages, there are a series of plots comparing the data to the simulation. The datasets and selections used to make these plots are the same as described earlier in this note, except as noted in the captions. Most of the exceptions are that the variable plotted is not cut on when making the histogram, ("N - 1" plots). This is dataset zewk6m compared to dataset bhmu0d, which has data before the August 2004 shutdown.

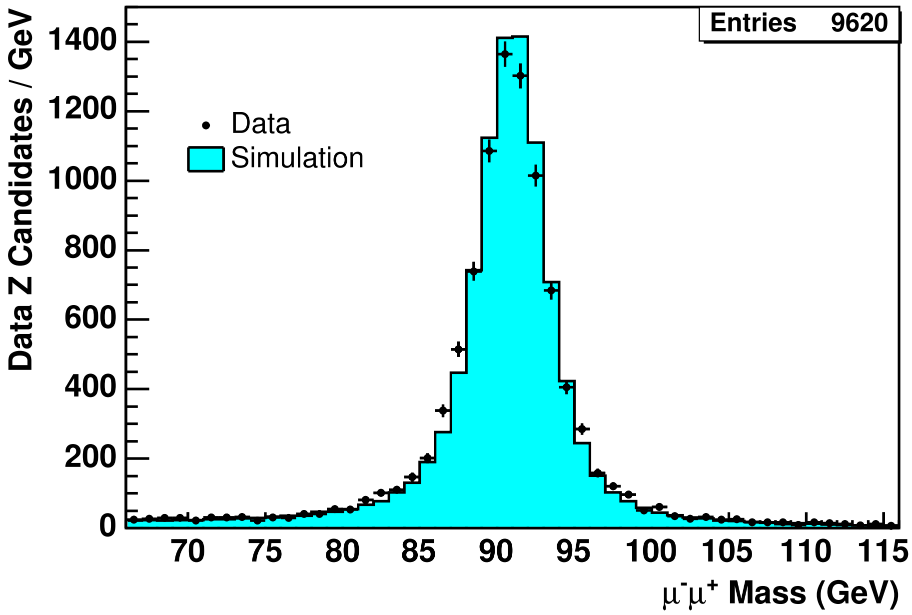

Figure 15: Reconstructed Z mass of candidates passing all selections.

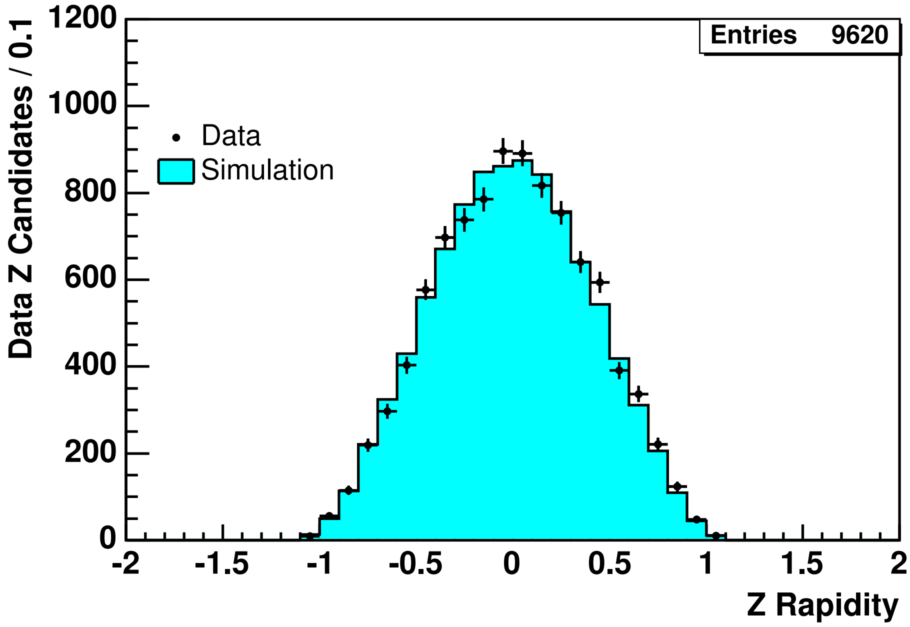

Figure 16: Reconstructed Z rapidity of candidates passing all selections.

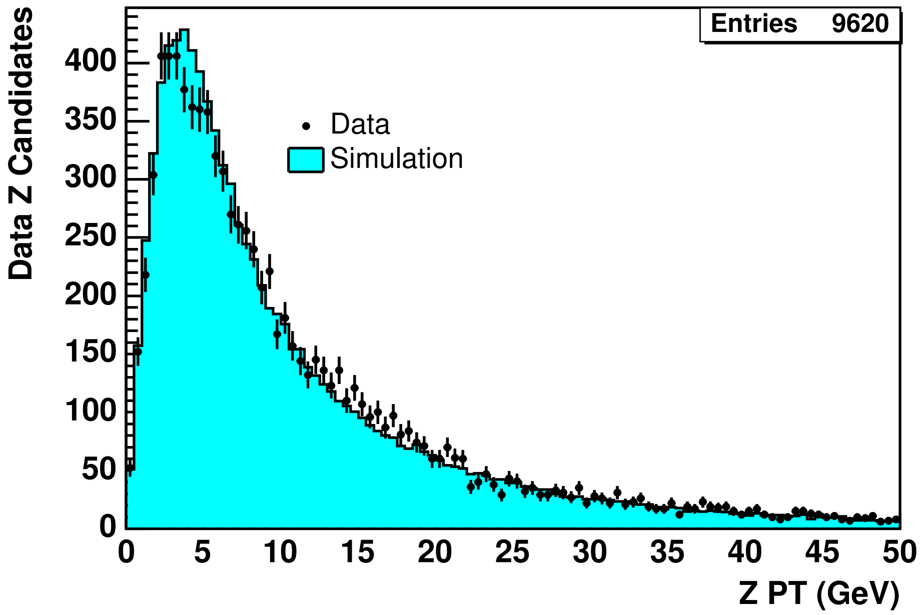

Figure 17: Reconstructed Z p_T of candidates passing all selections. Not acceptance corrected or unsmeared.

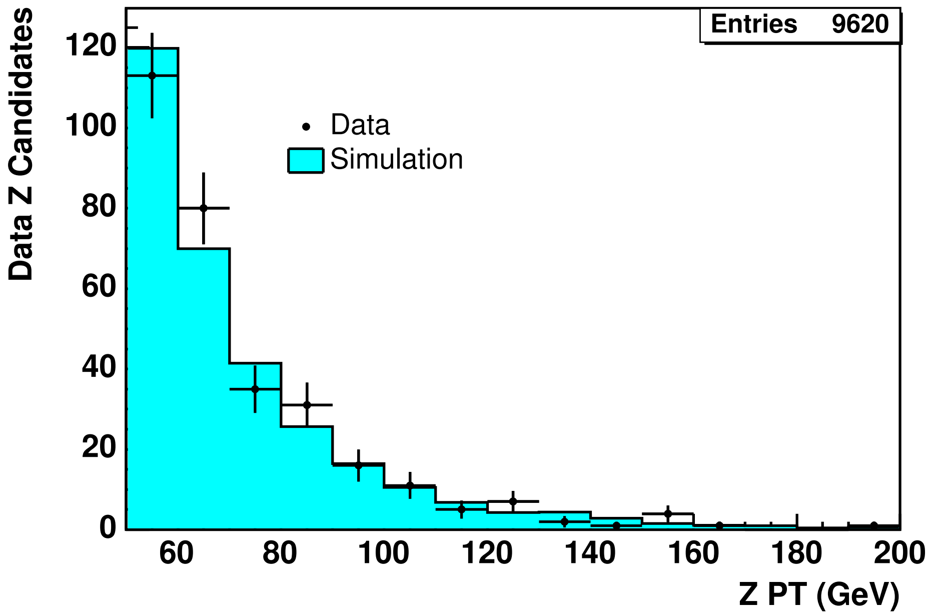

Figure 18: Reconstructed Z p_T of candidates passing all selections. Not acceptance corrected or unsmeared.

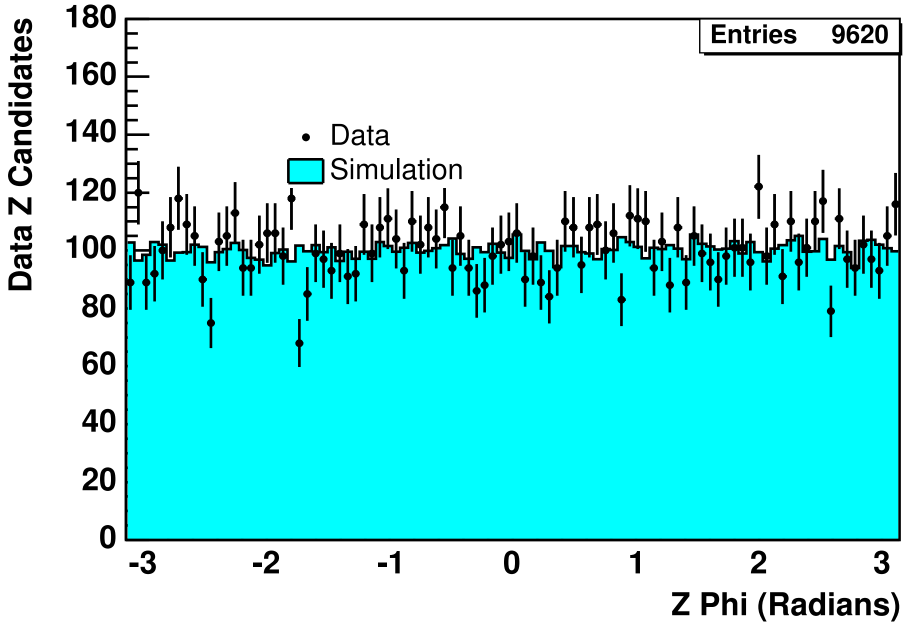

Figure 19: Reconstructed Z ϕ of candidates passing all selections.

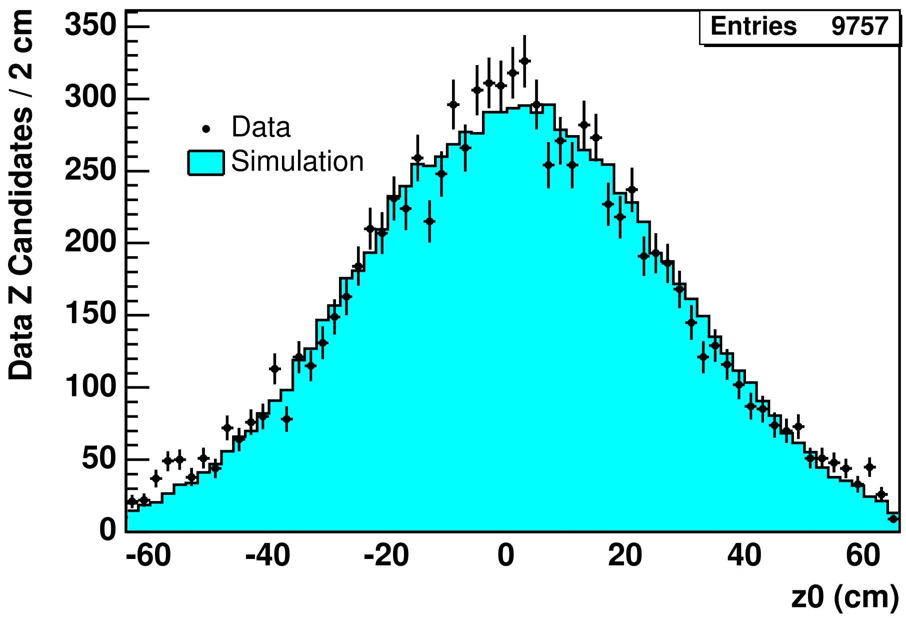

Figure 20: Reconstructed z_0 of candidates passing all selections except the $z_0 < 60$ cm cut. Average of two tracks z_0.

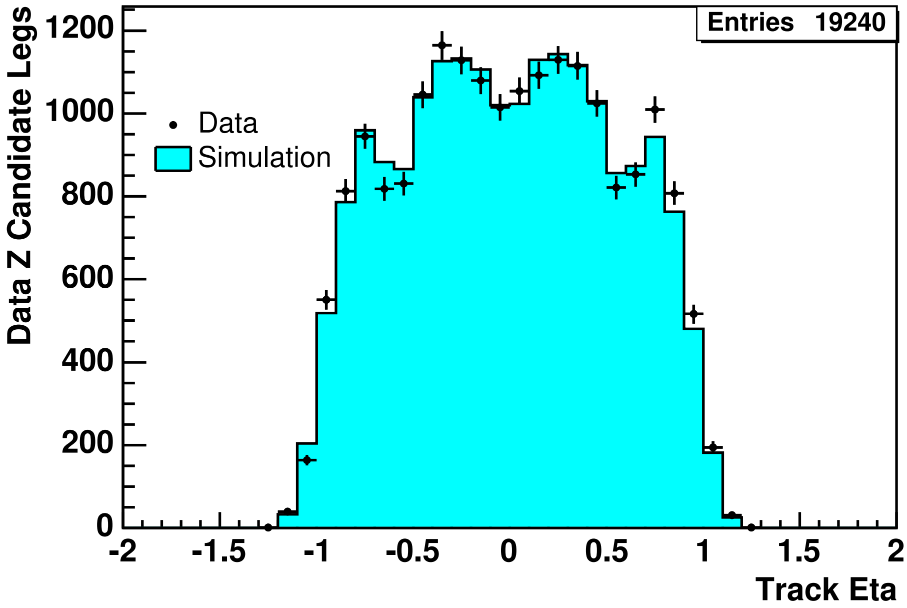

Figure 21: Reconstructed η of the tracks forming the Z candidates which pass all selections. One entry for each track.

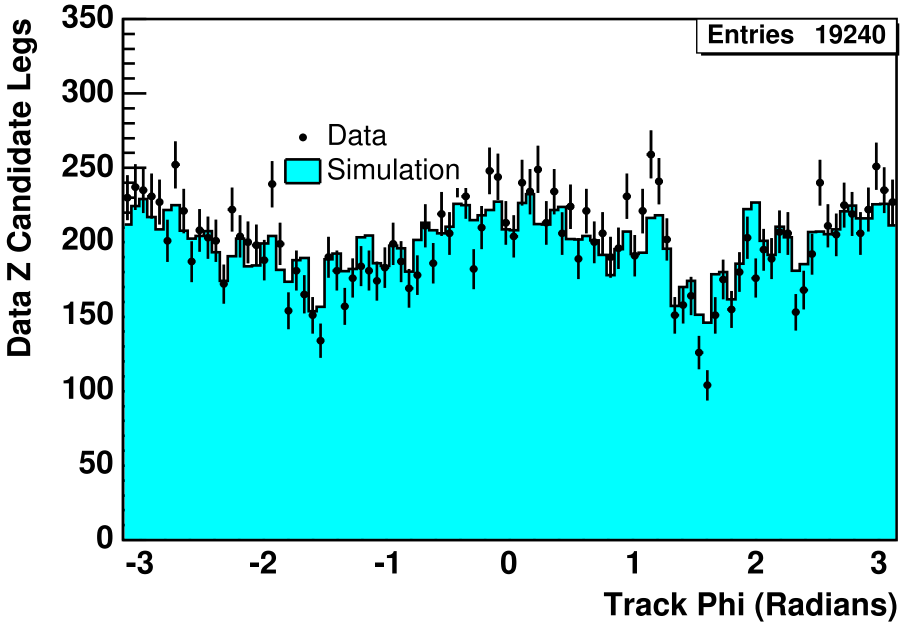

Figure 22: Reconstructed ϕ of the tracks forming the Z candidates which pass all selections One entry for each track.

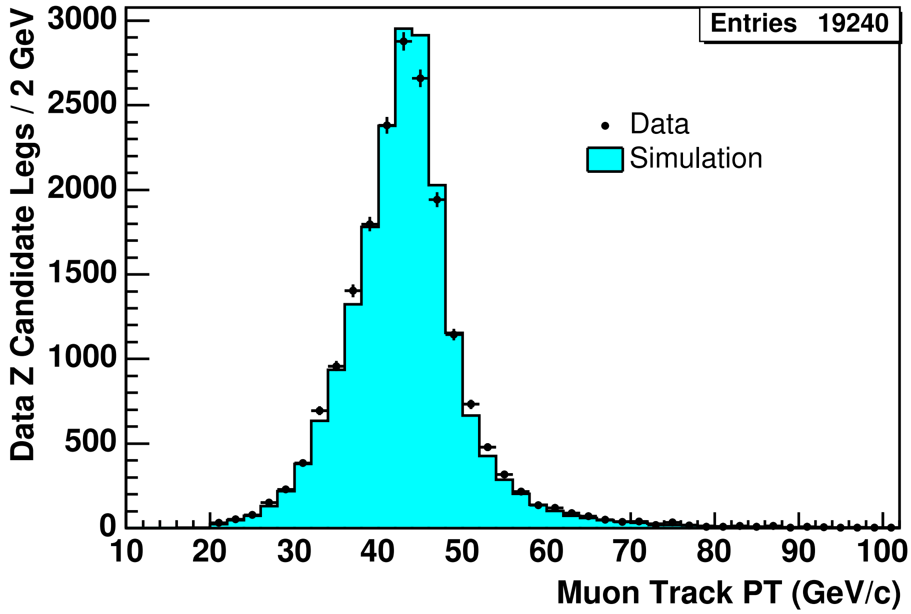

Figure 23: Reconstructed p_T of the tracks forming the Z candidates which pass all selections. One entry for each track.

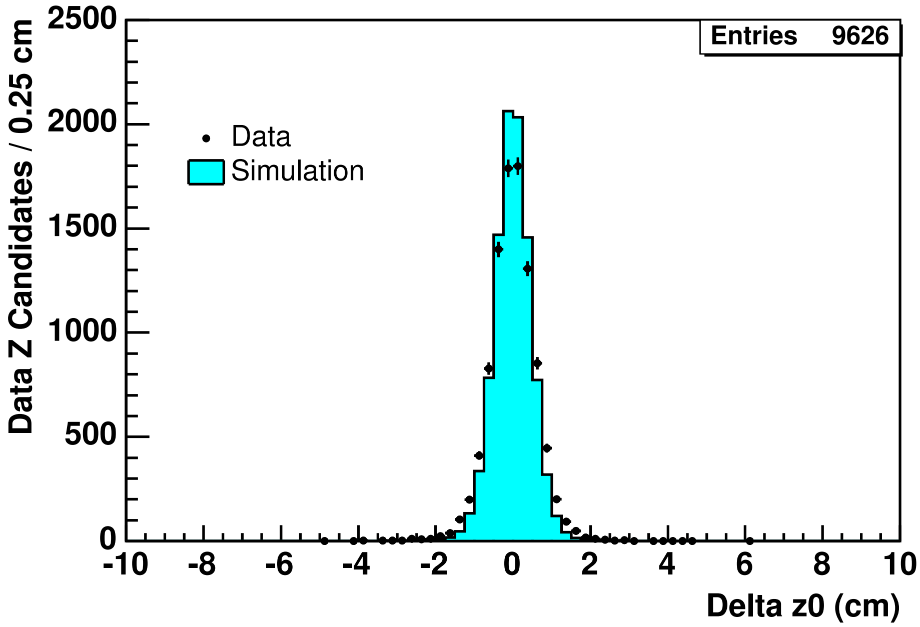

Figure 24: Reconstructed Δz_0 between the two tracks forming the Z candidates which pass all selections except the cut on Δz_0.

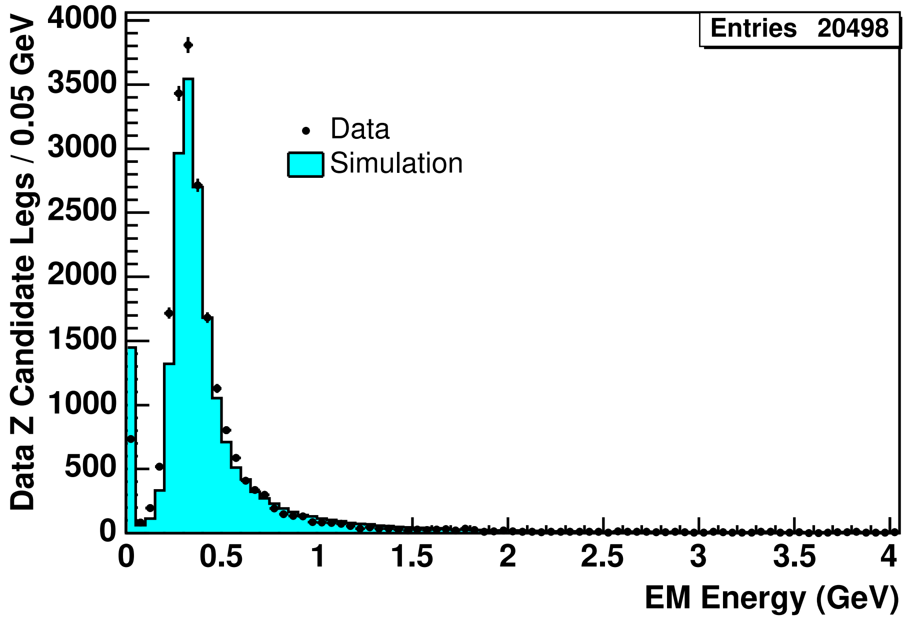

Figure 25: Reconstructed EM energy of the tracks forming the Z candidates which pass all selections, except the EM cut.

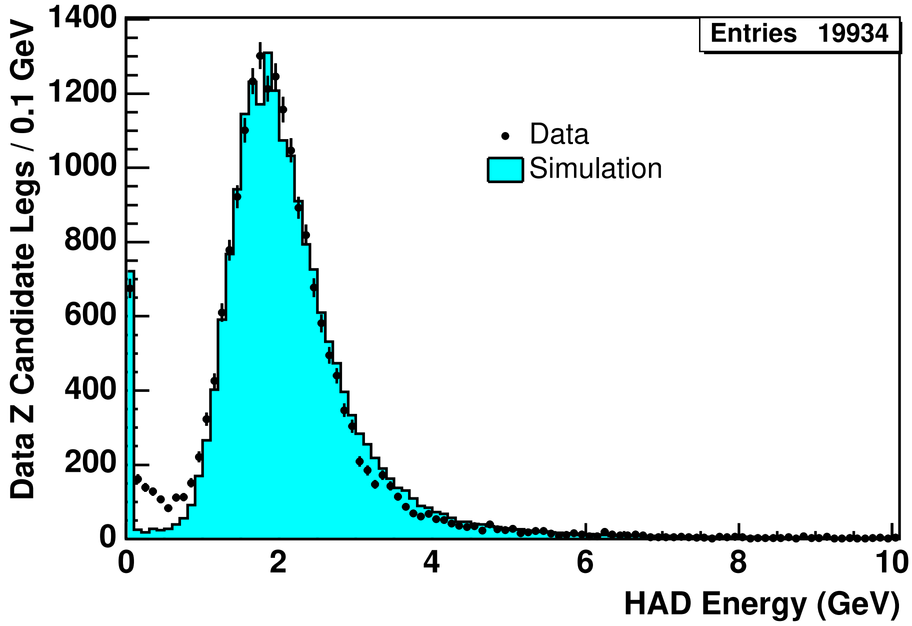

Figure 26: Reconstructed HAD energy of the tracks forming the Z candidates which pass all selections, except the HAD cut.

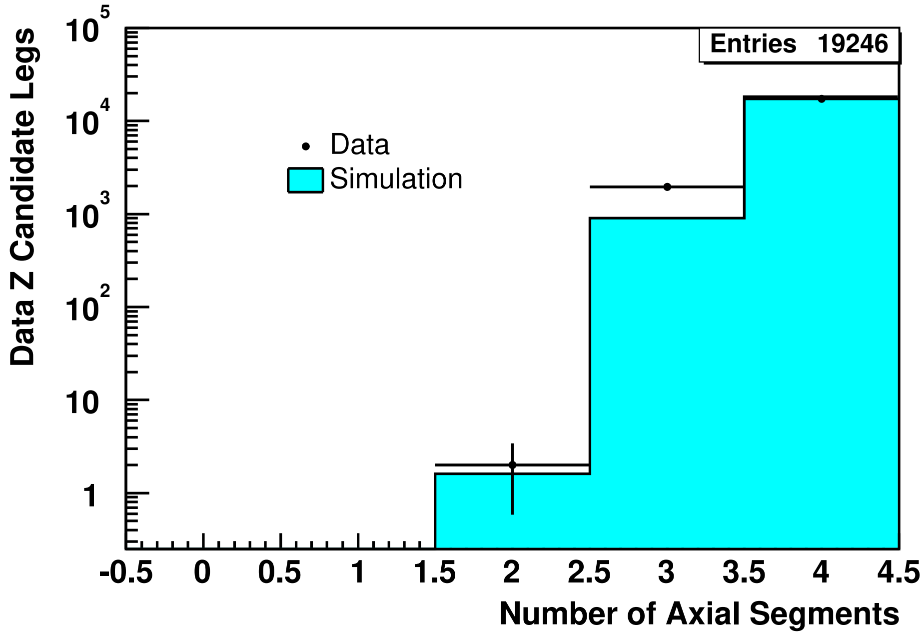

Figure 27: Number of axial segments on the tracks forming the Z candidates which pass all selections, except both segment cuts.

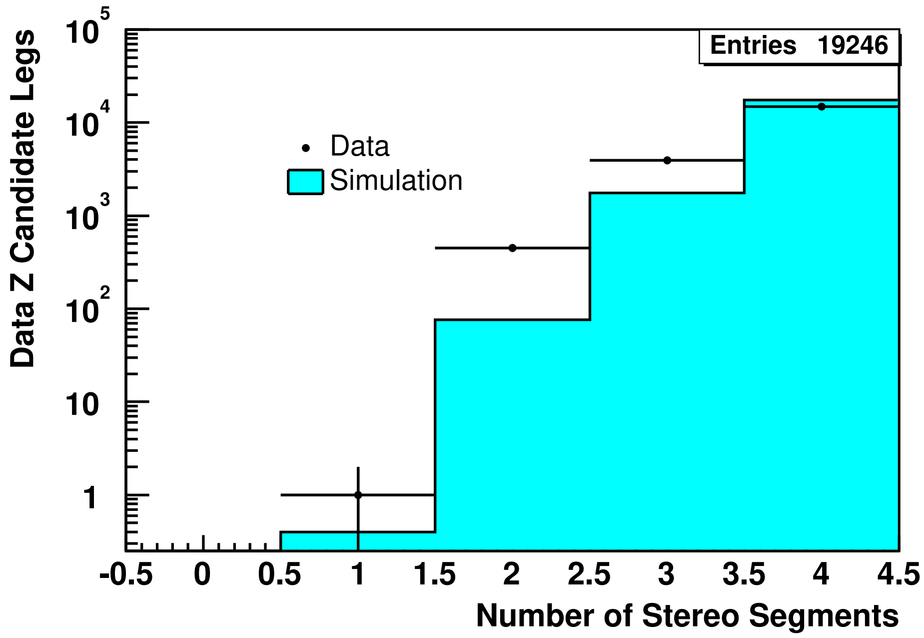

Figure 28: Number of stereo segments on the tracks forming the Z candidates which pass all selections, except both segment cuts.

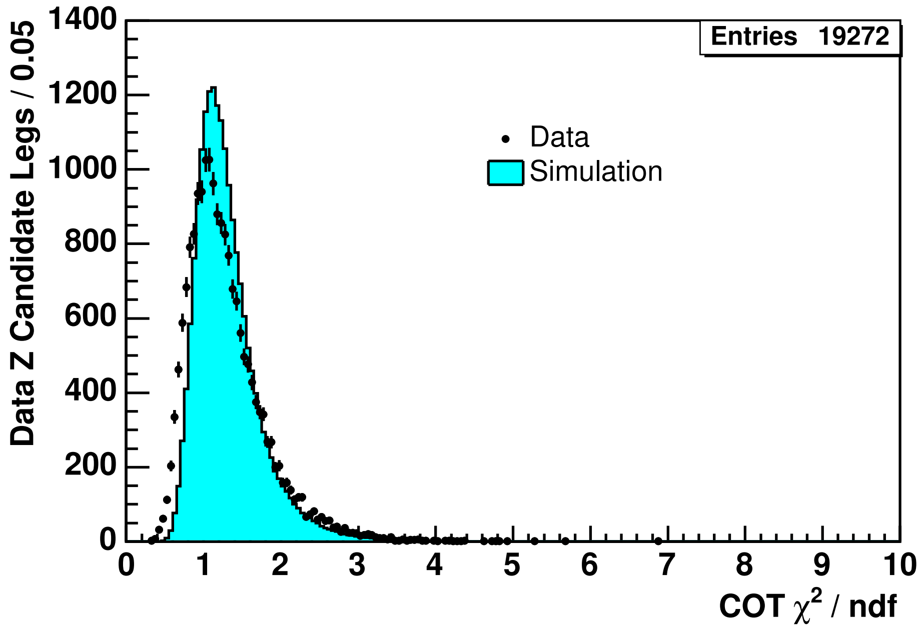

Figure 29: Reconstructed χ^2/ndf of the tracks forming the Z candidates which pass all selections, except the χ^2/ndf cut.

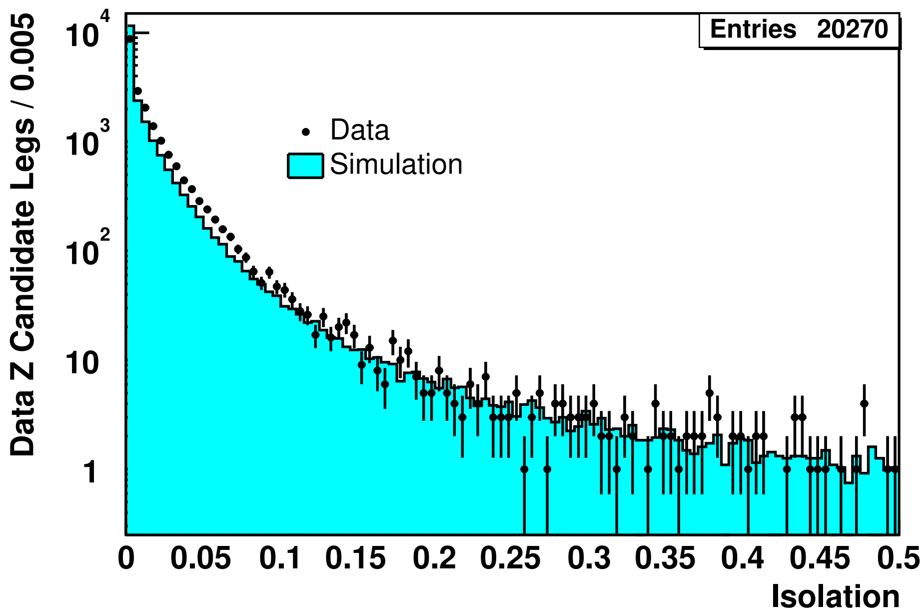

Figure 30: Isolation/p_T of the tracks forming the Z candidates which pass all selections, except the isolation/p_T cut.

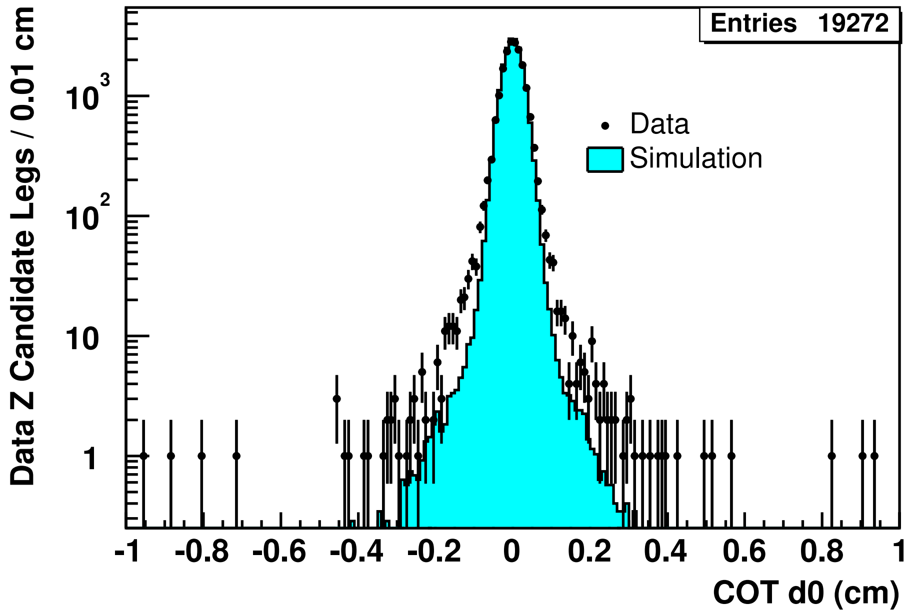

Figure 31: Reconstructed COT impact parameter of the tracks forming the Z candidates which pass all selections, except any impact parameter cuts.

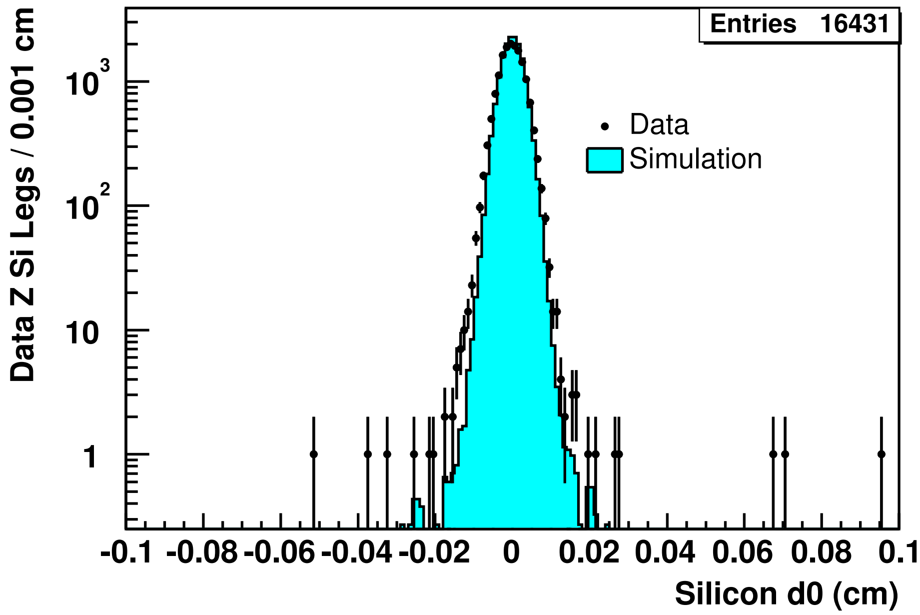

Figure 32: Reconstructed silicon impact parameter of the tracks forming the Z candidates which pass all selections, except any impact parameter cuts.

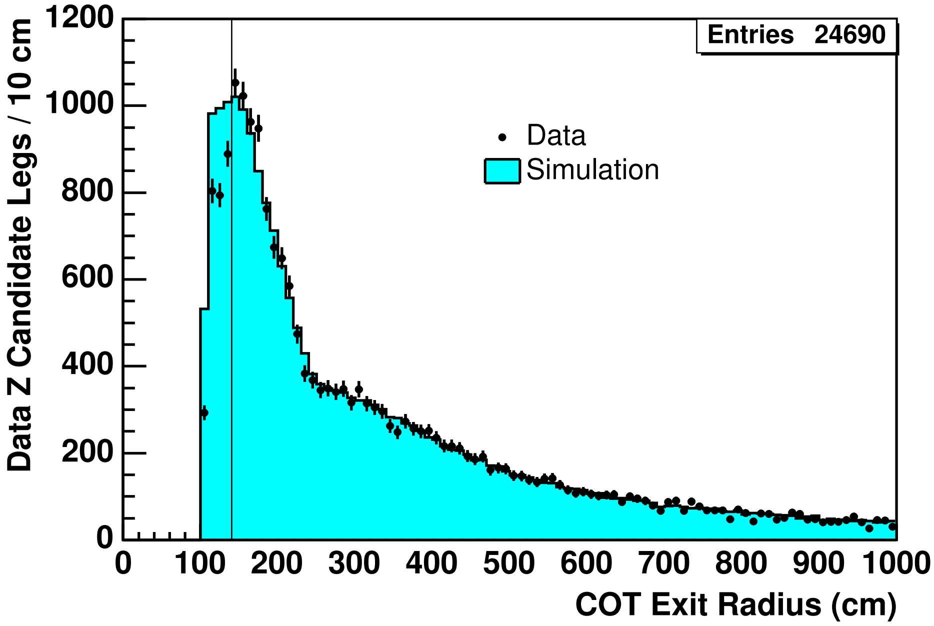

Figure 33: Reconstructed COT exit radius of the tracks forming the Z candidates which pass all selections, except the COT exit radius cut.

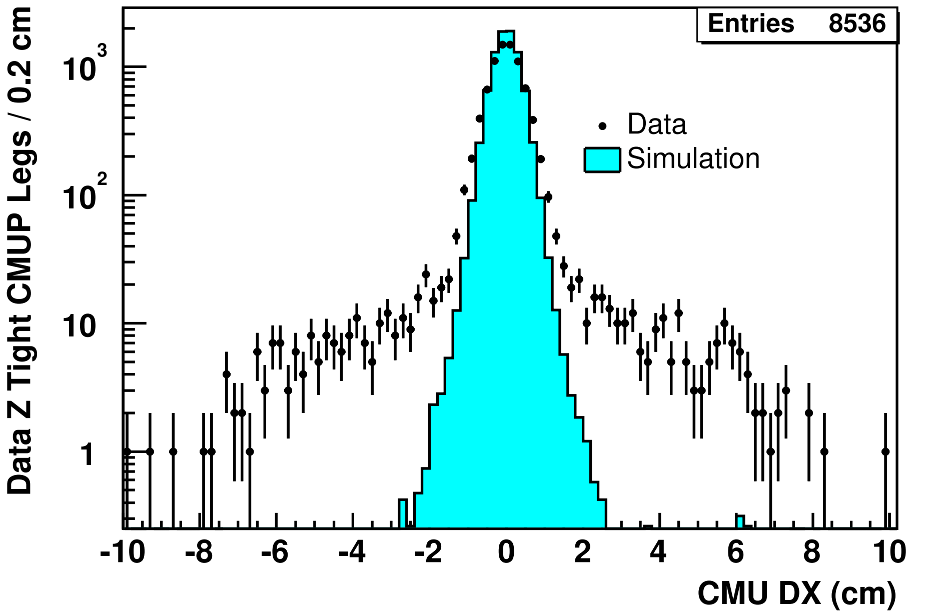

Figure 34: Reconstructed CMU DX of the tracks forming the Z candidates which pass all selections, except any CMU DX cuts. The tracks must also pass the tight CMUP selections, excluding the CMU DX cut.

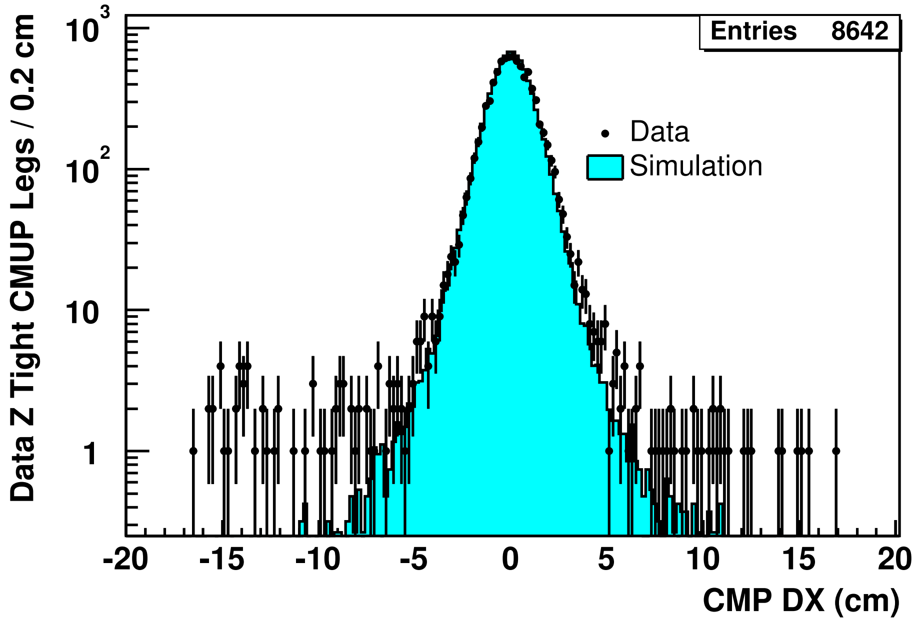

Figure 35: Reconstructed CMP DX of the tracks forming the Z candidates which pass all selections, except any CMP DX cuts. The tracks must also pass the tight CMUP selections, excluding the CMP DX cut.

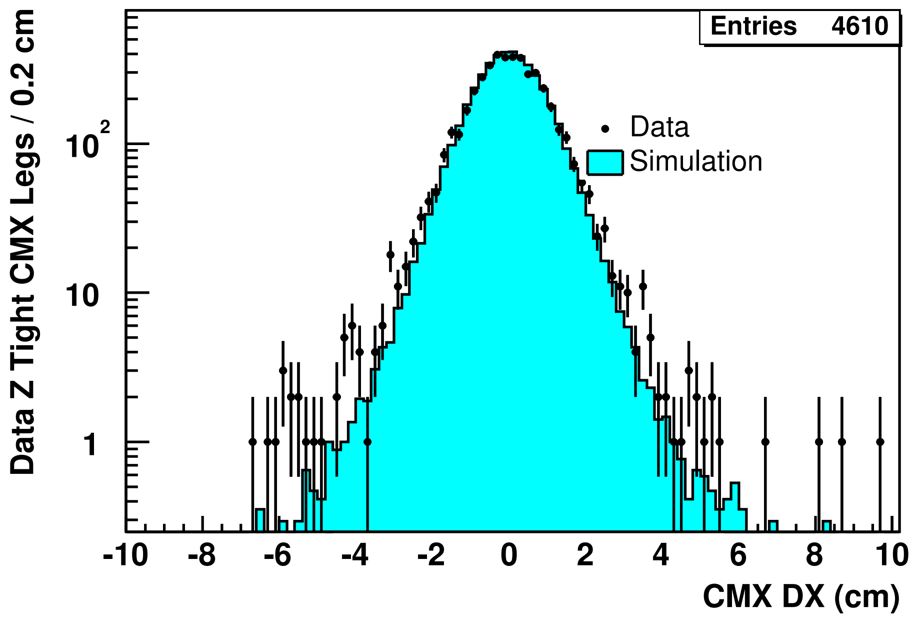

Figure 36: Reconstructed CMX DX of the tracks forming the Z candidates which pass all selections, except any CMX DX cuts. The tracks must also pass the tight CMX selections, excluding the CMX DX cut.

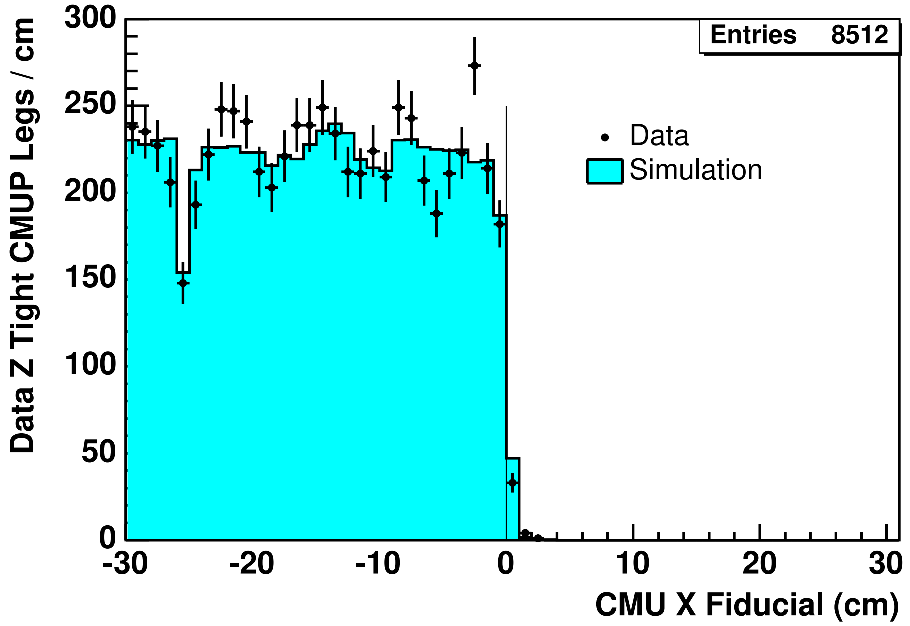

Figure 37: Reconstructed CMU X fiducial distance for the tracks forming the Z candidates which pass all selections, except the CMU X fiducial cut. The tracks must also pass the tight CMUP selections, excluding the CMU X fiducial cut.

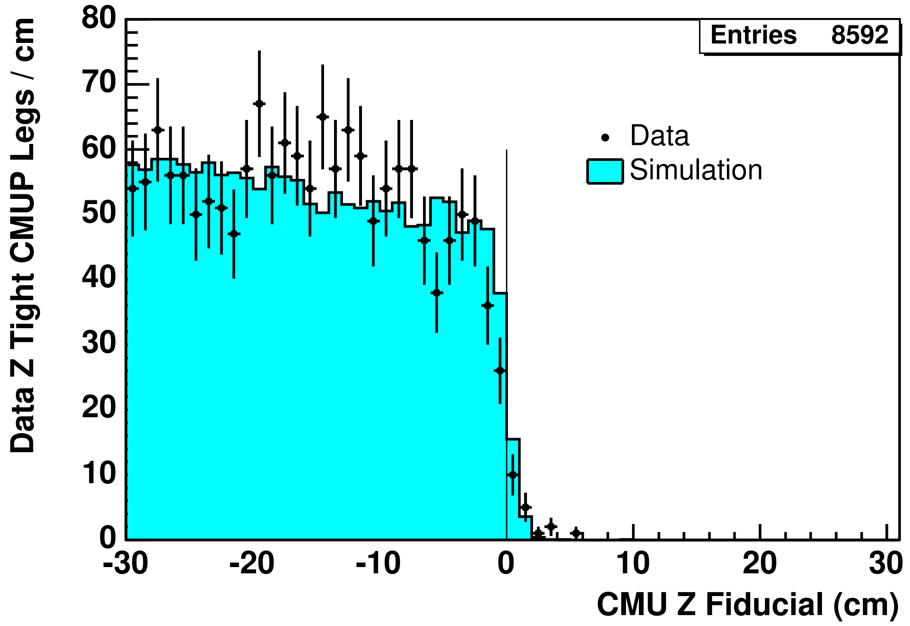

Figure 38: Reconstructed CMU Z fiducial distance for the tracks forming the Z candidates which pass all selections, except the CMU Z fiducial cut. The tracks must also pass the tight CMUP selections, excluding the CMU Z fiducial cut.

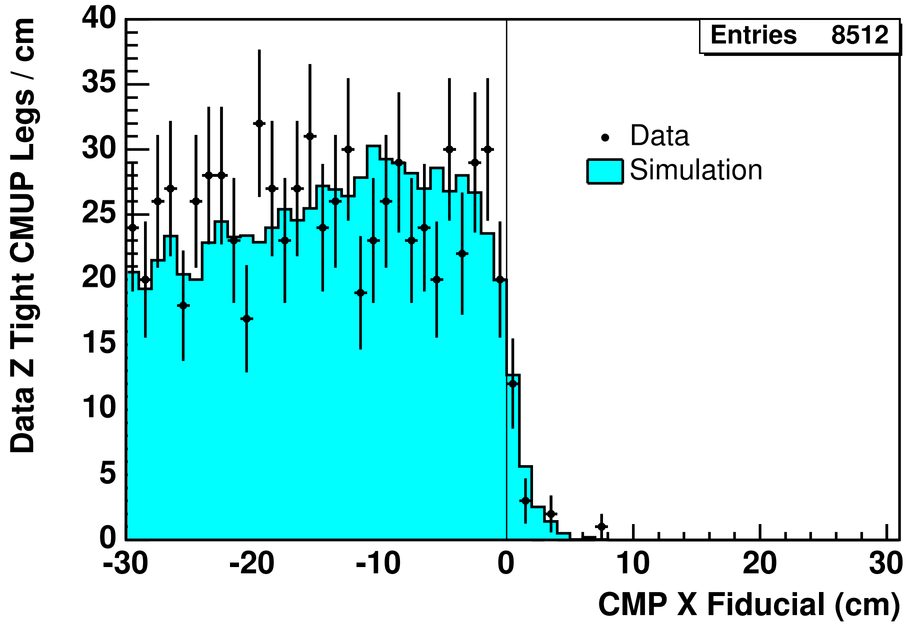

Figure 39: Reconstructed CMP X fiducial distance for the tracks forming the Z candidates which pass all selections, except the CMP X fiducial cut. The tracks must also pass the tight CMUP selections, excluding the CMP X fiducial cut.

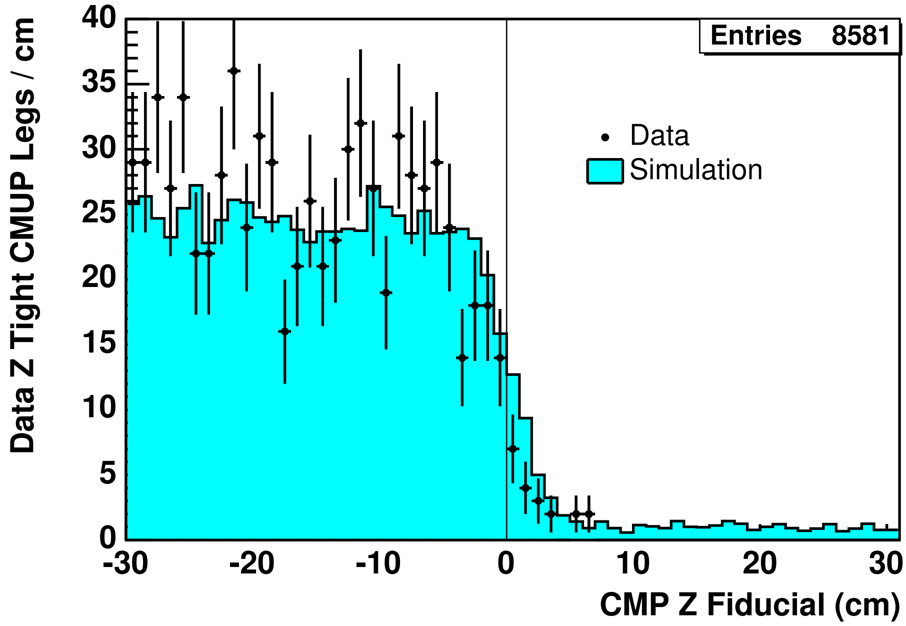

Figure 40: Reconstructed CMP Z fiducial distance for the tracks forming the Z candidates which pass all selections, except the CMP Z fiducial cut. The tracks must also pass the tight CMUP selections, excluding the CMP Z fiducial cut. Tail caused by bug in CMP geometry near detector feet which has been fixed in release 6.1.3.

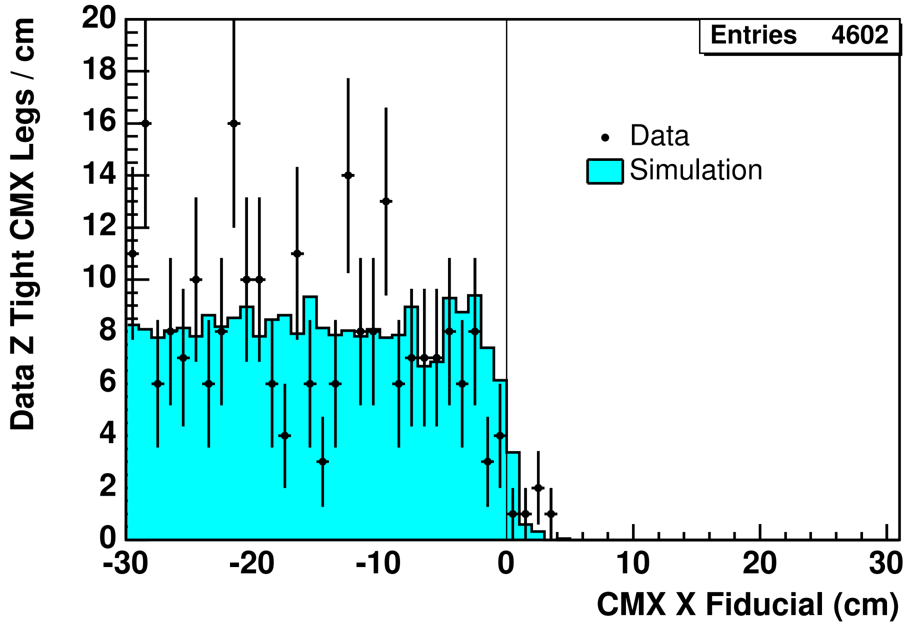

Figure 41: Reconstructed CMX X fiducial distance for the tracks forming the Z candidates which pass all selections, except the CMX X fiducial cut. The tracks must also pass the tight CMX selections, excluding the CMX X fiducial cut.

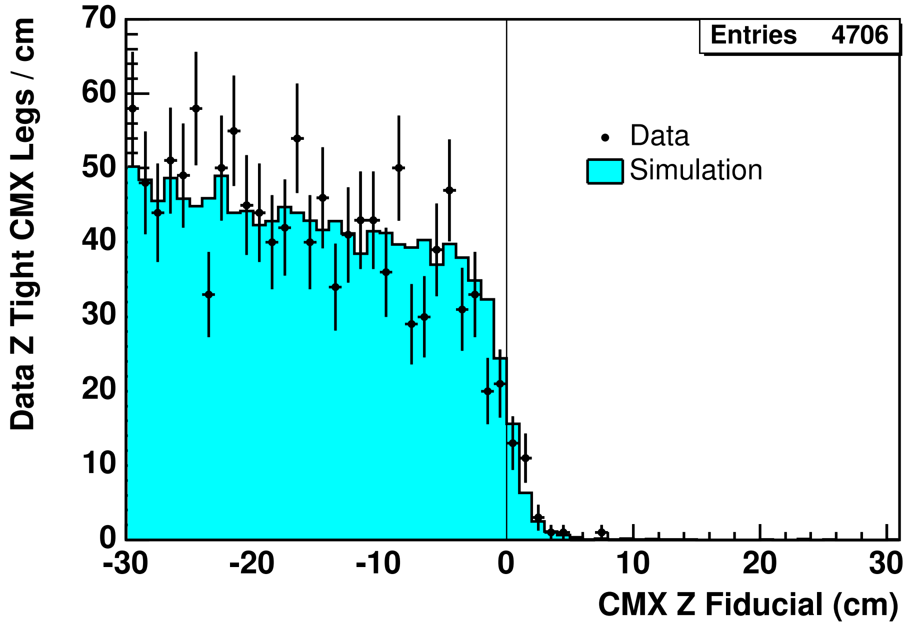

Figure 42: Reconstructed CMX Z fiducial distance for the tracks forming the Z candidates which pass all selections, except the CMX Z fiducial cut. The tracks must also pass the tight CMX selections, excluding the CMX Z fiducial cut.

8 Efficiencies

8.1 Vertex Efficiency

The requirement that the z coordinate of the interaction vertex be within 60 cm of z = 0 removes a significant fraction of the Z bosons in the data. We account for this with the vertex efficiency calculated by Willis Sakumoto. See CDF note 7324 for details of this calculation [13]. To be explicit, we use Z vertex efficiency = 0.951 ± 0.003.

8.2 Tracking Efficiency Scale Factor

We use the same tracking efficiency scale factor used in the 72.0 pb^{-1} analysis [1]. This in turn relies on the tracking efficiency calculation documented in CDF Note 5973 [14]. The measurement is based on the "W no track" sample of $W \to e\nu$ events. A sample of pure electrons is selected and the fraction of these with a matching COT track is evaluated. A scale factor is calculated by taking the ratio of the tracking efficiency in data to the tracking efficiency in simulation. The tracking efficiency in the data is measured to be $0.9963^{+0.0035}_{-0.0040}$. The efficiency in the simulation is measured to be $0.9966^{+0.0015}_{-0.0024}$. The scale factor is 1.000 ± 0.004.

8.3 Muon ID, Isolation, Muon Reconstruction, and Muon Trigger Efficiencies

We measure the efficiencies of the muon ID, isolation, muon reconstruction, and muon trigger Z selection requirements. We define the muon ID requirements as the requirements on E_{EM}, E_{HAD}, dx, the number of COT segments, d_0, and the COT track χ^2/ndf. The muon reconstruction efficiency is the probability a stub or stubs will be associated to a muon given that the muon is already associated to a COT track that extrapolates to the muon detectors. Section 5 discusses the selection requirements for the Z signal candidates in detail.

8.3.1 The Method

To determine the effect a selection requirement or cut has on the Z cross section, we measure its efficiency and the corresponding uncertainty with the following formulas:

$$\epsilon = \frac{N_{pass}}{N_{pass} + N_{fail}}, \tag{1}$$

$$\sigma_\epsilon = \frac{1}{N_{pass} + N_{fail}} \sqrt{\sigma^2_{N_{pass}} (1-\epsilon)^2 + \sigma^2_{N_{fail}} \epsilon^2}. \tag{2}$$

N_{pass} is the number of muons that pass the cut and N_{fail} is the number of muons that fail the cut. The uncertainties are based on the Poisson uncertainties on the number that pass and fail. This sounds simple so far, but there are a lot of details related to selecting a sample of muons to use to derive N_{pass} and N_{fail}.

We start with the same dataset and runs used to select our Z signal. These runs have all passed data quality checks on the relevant detectors: CMU, CMP, CMX, COT, the

Trigger Leg Requirements
All trigger leg cuts in Z signal selection
See Tables 3 and 4
CMUP or CMX
Test Leg Requirements
COT only track or has a COT only parent
Successfully passes beam constrained refit
Not an IO or silicon only track
p_T
Not a cosmic
ρ_{COT}
E_{EM}
E_{HAD}
CMU and CMP Fiducial Cuts for CMUP efficiency
CMX Fiducial Cuts for CMX efficiency
Other Requirements
Z mass 80 to 100 GeV
$\lvert z_0 \rvert$
$\lvert \Delta z_0 \rvert$
Opposite charge
For simulation, generated and reconstructed Z must match

Table 7: Selection requirements for the muon reconstruction efficiency measurement. If the cutoff is the same as in the Z signal selection, it is not repeated here (see Tables 3, 4, and 5). But if the cutoff is different, then it is shown here.

calorimeters, and others. Using the same runs ensures the efficiencies are time averaged properly, because they vary a little with time.

We select muons from the two legs of Z candidates, although the cuts used to select the Z candidates are modified and not the same as used to determine the Z signal for the cross section calculation. We arbitrarily select one leg of a Z candidate as a trigger leg and another leg as a test leg. The trigger leg must pass one set of requirements and the test leg must pass another set of requirements. There are also other requirements on the Z candidate. If the candidate passes all the requirements, then N_{pass} or N_{fail} is incremented based on whether the test leg passes the cut. The process is repeated with the assignment of the two muons reversed, the trigger leg becomes the test leg and vice versa. This is similar to the procedure used many times in the past to measure these efficiencies. For example, see CDF Note 7367 [7].

These efficiencies are divided into 3 cases. For the muon reconstruction efficiencies, we use the selections in Table 7 to select the muons used to measure the efficiency. For the muon ID and isolation efficiencies, we use the selections in Table 8. For the trigger efficiencies, we use the selections in Table 9.

We try to order the calculation of the efficiencies as follows: muon reconstruction then muon ID except dx, then isolation, then dx, and finally muon trigger. Practically, this means

Trigger Leg Requirements
COT only track or has a COT only parent Successfully passes beam constrained refit Not an IO or silicon only track $p_T > 18.0$ Gev Not a cosmic $E_{EM} < \min(3, 3 + 0.0140 * (p - 100))$ $E_{HAD} < \min(9, 9 + 0.042 * (p - 100))$ Isolation / $p_T < 0.4$ d0
EITHER Has a CMU stub and a CMP stub, bluebeam veto CMU $\|dx\| < 5$ cm and CMP $\|dx\| < 10$ cm CMUP trigger
OR Has a CMX stub, keystone and miniskirt veto CMX $\|dx\|$ CMX trigger
Test Leg Requirements
COT only track or has a COT only parent Successfully passes beam constrained refit Not an IO or silicon only track p_T Not a cosmic ρ_{COT}
For CMUP efficiencies: Has a CMU stub and a CMP stub, bluebeam veto CMU and CMP Fiducial Cuts
For CMX efficiencies: Has a CMX stub, miniskirt and keystone veto CMX Fiducial Cuts
Other Requirements
Z mass 66 to 116 GeV $\|z_0\|$ $\|\Delta z_0\|$ Opposite charge For simulation, generated and reconstructed Z must match

Table 8: Selection requirements for the muon ID and isolation efficiency measurements. If the cutoff is the same as in the Z signal selection, it is not repeated here (see Tables 3, 4, and 5). But if the cutoff is different, then it is shown here. See comments in the text for some addition cuts made on the test leg when measuring some of these efficiencies.

Trigger Leg Requirements
All trigger leg cuts in Z signal selection See Tables 3 and 4 For L1 measurements, can be CMUP or CMX For L3 CMUP efficiency measurement, must be CMX For L3 CMX efficiency measurement, must be CMUP
Test Leg Requirements
All trigger leg cuts in Z signal selection EXCEPT trigger cut See Tables 3 and 4 Require CMUP case when measuring CMUP trigger efficiency Require CMX case when measuring CMX trigger efficiency Add L1 requirement when measuring L3 efficiencies
Other Requirements
Z mass 80 to 100 GeV $\|z_0\|$ $\|\Delta z_0\|$ Opposite charge

Table 9: Selection requirements for the muon trigger efficiency measurement. If the cutoff is the same as in the Z signal selection, it is not repeated here (see Tables 3, 4, and 5). But if the cutoff is different, then it is shown here.

that when measuring the efficiency for a cut, all the preceding cuts have been made on the test leg before counting the passing and failing muons.

One exception to the ordering is that when calculating the muon reconstruction efficiency, we cut on E_{EM} and E_{HAD}. We believe the correlation between these cuts and the muon reconstruction efficiency is small. From studying the same sign events, we see that the cuts remove a small but measurable amount of background. The background is a larger problem than the correlations so we make the cut.

When measuring efficiencies used for the cross section calculation, we measure all the muon ID efficiencies and the isolation efficiency together as one combined efficiency. Only the dx efficiency is measured separately. When the dx efficiency is measured, all the other muon ID cuts and the isolation cut are made before calculating N_{pass} and N_{fail}. Although we do not use the results, we also calculate the other muon ID efficiencies individually without any additional cuts. We also calculate the isolation efficiency individually, but after making all the muon ID cuts except for the dx cut.

For the muon ID and isolation efficiencies we established our cuts by starting with the method documented in CDF note 6711 and making the following changes.

1. We widened the Z mass window from 80:100 GeV to 66:116 GeV. The narrow window creates a bias on the efficiency of order 1 %. Radiation causes candidates to have low mass. Radiation also cause events to fail the EM and isolation cuts. A narrow mass range eliminates the events most likely to fail the cuts.

2. We add a loose isolation / p_T < 0.4 cut. This removes a significant fraction of the

background but does not remove many good Z boson candidates from the sample used to measure the efficiency.

3. We add a d0 cut on the first leg. There are a few cosmics left in the sample used to measure the efficiencies and this eliminates a significant fraction of them.

4. We tighten the CMX dx cut to 6 cm, just because that is a more reasonable value than 20 cm.

More recent measurements of muon ID efficiencies have used even tighter cuts [7]. We are concerned about small biases that might be created by these tighter cuts. Although, we did not measure any with the cuts with we use. For example, there is a known correlation between the efficiency for the COT track χ^2 on the two legs. These tighter cuts are not necessary to eliminate background so we do not use them. Most of the background rejection comes from the isolation and d0 cuts which we discuss above.

8.3.2 The Results

The efficiencies measured from the data are shown in Table 10. The efficiencies measured from the simulation are shown in Table 11. Table 12 duplicates the information in the two preceding tables, but is organized so the data and simulation efficiencies can be compared. The "scale factor" or ratio of data efficiency to simulation efficiency is also shown.

The background that is most likely to bias the efficiency measurements is the same sign background related to jets. Table 10 shows the number of same sign background events in the samples used to measure the efficiencies. In the largest cases, the number of same sign candidates is of order 1 part in a thousand. This is 3 or 4 times smaller the statistical uncertainties in the efficiency calculations and therefore ignored. Other backgrounds are less of a problem, because they mostly consist of real muons. Background containing real muons does not increase much with the looser cuts used to measure the efficiency. In addition, these real muons should have efficiencies similar to the muons from Z decay which would minimize any potential bias.

We compared these efficiencies to those measured in CDF Note 6711 and the more recent CDF Note 7367 and find:

- The E_{HAD}, χ^2, CMP dx, CMX dx, CMX L1 trigger, and both L3 trigger efficiencies which were previously measured are all consistent with our measurements.

- The segment, d_0, and CMU dx efficiencies we measure are higher because we have loosened these cuts and expect higher efficiencies.

- The E_{EM} and isolation efficiencies we measure are lower because we have used a Z mass window from 66 to 116 GeV when measuring the efficiencies. The 80 to 100 GeV window used in the older measurements created a bias.

- We measure different muon reconstruction efficiencies, because we use modified muon fiducial cuts. But the corresponding scale factors shown in Table 12 are consistent with the previously measured scale factors.

Cut	Events (CMUP)	Efficiency (CMUP)	Events (CMX)	Efficiency (CMX)
Same Sign	7		4	
Opposite Sign	5989		3091	
E_{EM}	5767	0.9629 ± 0.0024	2999	0.9702 ± 0.0031
E_{HAD}	5872	0.9805 ± 0.0018	3023	0.9780 ± 0.0026
Segments	5986	0.9995 ± 0.0003	3089	0.9994 ± 0.0005
d_0	5983	0.9990 ± 0.0004	3090	0.9997 ± 0.0004
χ^2/ndf	5980	0.9985 ± 0.0005	3090	0.9997 ± 0.0004
Track ID	5648	0.9431 ± 0.0030	2933	0.9489 ± 0.0040
Track ID plus iso	5509	0.9199 ± 0.0035	2874	0.9298 ± 0.0046
Same Sign	0		0	
Opposite Sign	5509		2874	
CMU DX	5482	0.9951 ± 0.0009		
CMP DX	5421	0.9840 ± 0.0017		
CMU and CMP DX, CMX DX	5394	0.9791 ± 0.0019	2866	0.9972 ± 0.0010
Same Sign	1		0	
Opposite Sign	5648		2933	
Isolation	5509	0.9754 ± 0.0021	2874	0.9799 ± 0.0026
Same Sign	5		0	
Opposite Sign	5421		2506	
Muon Reconstruction	4742	0.8747 ± 0.0045	2456	0.9800 ± 0.0028
Same Sign	0		0	
Opposite Sign	4545		2404	
L1 Trigger	4104	0.9030 ± 0.0044	2322	0.9659 ± 0.0037
Same Sign	0		0	
Opposite Sign	1428		1424	
L3 Trigger	1424	0.9972 ± 0.0014	1424	1.0000 ± 0.0008

Table 10: Efficiencies calculated from data.

Cut	Events (CMUP)	Efficiency (CMUP)	Events (CMX)	Efficiency (CMX)
Opposite Sign	123694		60781	
E_{EM}	117960	0.9536 ± 0.0006	58153	0.9568 ± 0.0008
E_{HAD}	121592	0.9830 ± 0.0004	59406	0.9774 ± 0.0006
Segments	123687	0.9999 ± 0.0000	60774	0.9999 ± 0.0000
d_0	123665	0.9998 ± 0.0000	60763	0.9997 ± 0.0001
χ^2/ndf	123589	0.9992 ± 0.0001	60731	0.9992 ± 0.0001
Track ID	115832	0.9364 ± 0.0007	56778	0.9341 ± 0.0010
Track ID plus iso	113114	0.9145 ± 0.0008	55444	0.9122 ± 0.0011
Opposite Sign	113114		55444	
CMU DX	113100	0.9999 ± 0.0000		
CMP DX	112490	0.9945 ± 0.0002		
CMU and CMP DX, CMX DX	112483	0.9944 ± 0.0002	55355	0.9984 ± 0.0002
Opposite Sign	115832		56778	
Isolation	113114	0.9765 ± 0.0004	55444	0.9765 ± 0.0006
Opposite Sign	98897		45479	
Muon Reconstruction	91993	0.9302 ± 0.0008	44993	0.9893 ± 0.0005

Table 11: Efficiencies calculated from simulation.

- Our CMUP L1 trigger efficiency is roughly 1% lower than the previous measurements. We traced this difference to the change in the CMU dx cut. The events added by loosening the cut have a significantly lower chance to pass the trigger.

Cut	Efficiency Data	Efficiency Simulation	Scale Data / Simulation
E_{EM} - CMUP	0.9629 ± 0.0024	0.9536 ± 0.0006	1.0097 ± 0.0026
E_{EM} - CMX	0.9702 ± 0.0031	0.9568 ± 0.0008	1.0141 ± 0.0033
E_{HAD} - CMUP	0.9805 ± 0.0018	0.9830 ± 0.0004	0.9974 ± 0.0019
E_{HAD} - CMX	0.9780 ± 0.0026	0.9774 ± 0.0006	1.0006 ± 0.0028
Segments - CMUP	0.9995 ± 0.0003	0.9999 ± 0.0000	0.9996 ± 0.0003
Segments - CMX	0.9994 ± 0.0005	0.9999 ± 0.0000	0.9995 ± 0.0005
d_0 - CMUP	0.9990 ± 0.0004	0.9998 ± 0.0000	0.9992 ± 0.0004
d_0 - CMX	0.9997 ± 0.0004	0.9997 ± 0.0001	1.0000 ± 0.0004
χ^2/ndf - CMUP	0.9985 ± 0.0005	0.9992 ± 0.0001	0.9993 ± 0.0005
χ^2/ndf - CMX	0.9997 ± 0.0004	0.9992 ± 0.0001	1.0005 ± 0.0004
Track ID - CMUP	0.9431 ± 0.0030	0.9364 ± 0.0007	1.0071 ± 0.0033
Track ID - CMX	0.9489 ± 0.0040	0.9341 ± 0.0010	1.0158 ± 0.0044
Track ID plus iso - CMUP	0.9199 ± 0.0035	0.9145 ± 0.0008	1.0059 ± 0.0039
Track ID plus iso - CMX	0.9298 ± 0.0046	0.9122 ± 0.0011	1.0193 ± 0.0052
DX - CMU	0.9951 ± 0.0009	0.9999 ± 0.0000	0.9952 ± 0.0009
DX - CMP	0.9840 ± 0.0017	0.9945 ± 0.0002	0.9895 ± 0.0017
DX - CMU and CMP	0.9791 ± 0.0019	0.9944 ± 0.0002	0.9846 ± 0.0019
DX - CMX	0.9972 ± 0.0010	0.9984 ± 0.0002	0.9988 ± 0.0010
Isolation - CMUP	0.9754 ± 0.0021	0.9765 ± 0.0004	0.9988 ± 0.0022
Isolation - CMX	0.9799 ± 0.0026	0.9765 ± 0.0006	1.0035 ± 0.0027
Muon Reconstruction - CMUP	0.8747 ± 0.0045	0.9302 ± 0.0008	0.9404 ± 0.0049
Muon Reconstruction - CMX	0.9800 ± 0.0028	0.9893 ± 0.0005	0.9906 ± 0.0029

Table 12: Comparison of efficiencies calculated from data and simulation.

8.3.3 Combining the Many Efficiencies Into a Single Scale Factor

These efficiencies cannot be simply multiplied together because there are two legs in each Z candidate and some cuts are applied to both legs and some cuts to only one leg. There are also efficiencies measured in CMX and CMUP. There are also efficiencies measured in simulation and data. One needs to combine all these together into a single scale factor that accounts for all the efficiencies in a coherent way. The following formulas are used to do this.

$$
\begin{aligned}
\text{Numerator} = \\
& n_{11}\epsilon_{t1}^2(\epsilon_{s1}^2 + 2\epsilon_{s1}(1-\epsilon_{s1})) \\
& + n_{22}\epsilon_{t2}^2(\epsilon_{s2}^2 + 2\epsilon_{s2}(1-\epsilon_{s2})) \\
& + n_{12}\epsilon_{t1}\epsilon_{t2}(\epsilon_{s1}\epsilon_{s2} + \epsilon_{s1}(1-\epsilon_{s2}) + \epsilon_{s2}(1-\epsilon_{s1})) \\
& + n_{13}\epsilon_{t1}^2\epsilon_{s1} \\
& + n_{14}\epsilon_{t1}\epsilon_{t2}\epsilon_{s1} \\
& + n_{23}\epsilon_{t2}\epsilon_{t1}\epsilon_{s2} \\
& + n_{24}\epsilon_{t2}^2\epsilon_{s2},
\end{aligned}
$$

$$
\begin{aligned}
\text{Denominator} = \\
& n_{11}\epsilon_{t1'}^2(\epsilon_{s1'}^2 + 2\epsilon_{s1'}(1-\epsilon_{s1'})) \\
& + n_{22}\epsilon_{t2'}^2(\epsilon_{s2'}^2 + 2\epsilon_{s2'}(1-\epsilon_{s2'})) \\
& + n_{12}\epsilon_{t1'}\epsilon_{t2'}(\epsilon_{s1'}\epsilon_{s2'} + \epsilon_{s1'}(1-\epsilon_{s2'}) + \epsilon_{s2'}(1-\epsilon_{s1'})) \\
& + n_{13}\epsilon_{t1'}^2\epsilon_{s1'} \\
& + n_{14}\epsilon_{t1'}\epsilon_{t2'}\epsilon_{s1'} \\
& + n_{23}\epsilon_{t2'}\epsilon_{t1'}\epsilon_{s2'} \\
& + n_{24}\epsilon_{t2'}^2\epsilon_{s2'},
\end{aligned}
$$

$$\text{Scale Factor} = \text{Numerator}/\text{Denominator}.$$

In the above equations, all the "n" variables are counts of events in different categories, and all the "ϵ" variables are efficiencies. The subscripts denote the different kinds of counts or efficiencies. The sum of all the "n" variables is the total number of candidates passing all the selection requirements *except* for the requirements whose efficiency we have measured. The numerator is an estimate of the number of candidates passing all the selection requirements, where the estimate is made using efficiencies measured from the data. The denominator is the same thing, except the estimate is made using efficiencies measured from the simulation. The data to simulation ratio is the scale factor which is used to calculate the cross section.

n_{11} is the number of CMUP-CMUP candidates. n_{12} is the number of CMUP-CMX candidates. n_{22} is the number of CMX-CMX candidates. n_{13} is the number of CMUP-Track candidates, where the track is in the CMUP region. n_{14} is the number of CMUP-track candidates where the track is in the CMX region. n_{23} is the number of CMX-Track candidates, where the track is in the CMUP region. n_{24} is the number of CMX-Track candidates, where the track is in the CMX region.

Here are the details of how we count the candidates in these categories. We use the simulation. We start by selecting candidates that pass all the Z selection cuts described in Section 5 *except* for the cuts whose efficiency we are measuring. The cuts we do not make are the requirement of a linked muon stub, stub veto cuts (bluebeam, miniskirt, keystone), trigger requirements, d_0, E_{EM}, E_{HAD}, segment, χ^2, isolation, and dx requirements. If both legs of the remaining Z candidates are fiducial in both CMU and CMP we increment the n_{11} counter (the criteria is based on the muon fiducial cuts from Section 5). If both legs are fiducial in CMX, we increment n_{22}. If one leg is fiducial in CMU and CMP and the other leg is fiducial in CMX, we increment n_{12}. If none of the cases above are true, then we consider cases where only one of the legs is fiducial CMU and CMP or fiducial in CMX. The other leg we consider to be a "track" leg. We find the Z coordinate of the track at the radius of the CMU using this equation

$$z = z_0 + \lambda r,$$

where z_0 and λ are parameters of the track and r is 353.6 cm (the CMU radius). If |z| is less than 233 cm, the track is considered to be in the CMUP region, otherwise it is in the CMX region. If one leg is fiducial in CMU and CMP and the track leg is in the CMUP region, we increment n_{13}. If one leg is fiducial in CMU and CMP and the track leg is in the CMX region, we increment n_{14}. If one leg is fiducial in CMX and the track leg is in the CMUP region, we increment n_{23}. If one leg is fiducial in CMX and the track leg is in the CMX region, we increment n_{24}.

We use the data to derive efficiencies ϵ_{t1}, ϵ_{t2}, ϵ_{s1}, and ϵ_{s2}. We use the simulation to derive efficiencies $\epsilon_{t1'}$, $\epsilon_{t2'}$, $\epsilon_{s1'}$, and $\epsilon_{s2'}$. The efficiencies with an apostrophe in the subscript are derived with simulation and the others with data. The efficiencies with 1 in the subscript refer to efficiencies derived with a CMUP test leg and the efficiencies with a 2 in the subscript refer to efficiencies derived with a CMX test leg. The "t" and the "s" in the subscript refer to track and stub efficiencies. The track efficiencies are the "Track ID plus iso" efficiencies from Tables 10 and 11. "Track ID plus iso" efficiency refers to the probability to pass the d_0, segment, isolation, E_{EM}, E_{HAD}, and χ^2 cuts all together. For the data, the stub efficiency is the product of the muon reconstruction efficiency, the dx efficiency, and the trigger efficiency. For simulation, it is the product of the dx efficiency and the muon reconstruction efficiency. We do not simulate the trigger efficiency and it is not included in the stub efficiency for simulation.

It is simple to use the scale factor. It is in the denominator of the cross section formula. One important point related to this is that when calculating acceptances from the simulation we make all these cuts whose efficiency we have measured (except for the trigger efficiency). The scale factor corrects for discrepancies between data and simulation. The result of this calculation is that the scale factor is 0.9397 ± 0.0066.

Source of Systematic Uncertainty	Absolute Uncertainty	Relative Uncertainty (%)
PDF (positive)		1.72%
PDF (negative)		2.26%
Tracking Efficiency	1.000 ± 0.004	
(Tracking Efficiency)^2	1.000 ± 0.008	0.8%
NLO vs NNLO		0.72%
PYTHIA vs NNLO		0.36%
$\mathrm{d}\sigma/\mathrm{d}p_T$		0.08%
Momentum Scaling and Smearing		0.05%
Efficiency Scale Factor	0.9397 ± 0.0066	0.70%
Vertex Efficiency	0.951 ± 0.003	0.3%
Simulation Statistics	0.12209 ± 0.00028	0.2%
Background Estimate		negligible

Table 13: Summary of systematic uncertainties. Note the estimates in the first 8 lines above are taken directly from the 72 pb^{-1} analysis [3]. The efficiencies below the line were recalculated based on new data and/or simulation.

9 Systematic Uncertainties

Table 13 summarizes the systematic uncertainties. Several of them were calculated during the 72 pb^{-1} analysis and have not been recalculated. The uncertainties are taken directly from the submitted PRD article [3]. The details related to those uncertainty estimates are not repeated here. The reader is directed to Section V.E to Section V.I on pages 29 to 39 of [3]. In particular, Table XXII on page 39 and Table XII on page 31, show the results. Some brief comments on the calculation of these uncertainties are given below.

- PDF - The uncertainties related to the PDF's were estimated by using the 40 error PDF's from CTEQ and determining the variations these caused in the acceptances [3].
- As discussed earlier, the uncertainty on the tracking efficiency is from CDF Note 5973 [14]. This is based on a study on "W no track" events.
- NLO vs NNLO - This uncertainty covers the uncertainties in the NNLO cross section calculation using the assumption that any residual errors are less than the difference between acceptances calculated using the NLO and NNLO calculations [3].
- PYTHIA vs NNLO - This is based on the difference between the acceptance calculated using only PYTHIA and an acceptance calculated by folding a $\mathrm{d}\sigma/\mathrm{dy}$ distribution calculated from NNLO with a calculation of acceptance as a function of rapidity from PYTHIA [3]. In the 72 pb^{-1} analysis, the acceptance calculated with the NNLO calculation was used. The NNLO calculation is not used in this analysis and therefore included as an additional systematic. The NNLO calculation does not give the cross section as a function of Z p_T and will not be very useful in the $\mathrm{d}\sigma/\mathrm{d}p_T$ analysis.
- The variation in the acceptance for different Z $\mathrm{d}\sigma/\mathrm{d}p_T$ distributions is another source of uncertainty [3].

- The variation in the acceptance as the momentum of the muons is scaled and smeared is another source of uncertainty [3].
- The uncertainty on the efficiency scale factor is derived based on the Poisson errors on the number of events in the data and simulation used to calculate the efficiencies. The uncertainties are propagated by standard formulas through the calculation of the overall scale factor. Uncertainties on the efficiencies from the background and kinematical properties of the Z's in the samples used to measure the efficiency are ignored. When we get to 4 fb^{-1} the uncertainties on the efficiencies related to the background will become significant, but not with the current data.
- The uncertainty on the vertex efficiency is from Willis Sakumoto's note [13].
- Uncertainty from the number of simulated events are significantly smaller than the other uncertainties.
- The backgrounds are so small that the uncertainty on the background estimates are negligible.

N_Z		9620
N_B		8.1 ± 1.6 ($Z \rightarrow \tau\tau$)
A_Z		0.12209 ± 0.00028 (error only from simulation statistics)
ϵ_{tot}		0.894 ± 0.010
	ϵ_{scale}	0.9397 ± 0.0066
	$\epsilon_{tracking}$	1.000 ± 0.004
	ϵ_{vertex}	0.951 ± 0.003
$\int \mathcal{L}dt$		337 ± 20 pb^{-1}

Table 14: Values of the factors used to calculate the cross section. $\epsilon_{tot} = \epsilon_{scale} \cdot \epsilon^2_{tracking} \cdot \epsilon_{vertex}$. The uncertainty on the acceptance only includes the statistical uncertainty related to the number of simulated events. Some systematic uncertainties are not shown in this table, but were discussed in the previous section. The largest of these uncertainties is related to the PDFs.

10 The Total Cross Section

We calculate the total Z cross section using the formula

$$\sigma \cdot B(p\overline{p} \rightarrow Z/\gamma^* \rightarrow \mu\mu) = \frac{N_Z - N_B}{A_Z \cdot \epsilon_{tot} \cdot \int \mathcal{L}dt},$$

where N_Z is the number of Z candidates passing all the selections, N_B is the estimate of the number of background events, A_Z is the acceptance calculated from simulation, ϵ_{tot} includes the effect of all the efficiency and scale factors, and $\int \mathcal{L}dt$ is the integrated luminosity. The values of the factors used in the calculation are shown in Table 14 and have all been discussed earlier in this note. The result is $261.2 \pm 2.7\,^{+5.8}_{-6.9} \pm 15.1$ pb, with uncertainties shown in the order statistical then systematic then luminosity.

A Comparison to Previously Published Z $\sigma \cdot B$

	CMUP/CMX + Track	CMUP + Track	CMX + Track
Old Result Note 6711	248.9 ± 5.9	252.1 ± 6.8	252.2 ± 9.7
New	246.0 ± 5.9	250.9 ± 6.8	246.9 ± 9.5
Uncertainty on Difference	3.2	3.5	4.8

Table 15: $\sigma \cdot B(Z/\gamma^* \to \mu\mu)$ in pb with statistical errors. The new result is a release 5.3.x analysis designed to reproduce the older result as closely as possible. The results are consistent within uncertainties that are shown in the last row. These uncertainties are discussed in detail in the text and caused by statistical fluctuations.

As a cross check, we reproduced the published CDF result [2] derived from a 72 pb^{-1} data sample. We modified our analysis to be as similar as possible to the older analysis to reproduce the results. Then we made changes one step a time to go from the old analysis to the new. We show the affect of each change on the total $\sigma \cdot B$ in the following sections. The changes we made to our analysis to make it like the old are as follows:

- We used an identical good run list.
- Used the background estimate of 0.0075% from CDF Note 6711 [1].
- We attempted to emulate all the details of the old efficiency calculation which is documented in CDF Note 6711.
- We intentionally reproduced the effects of a small error in the luminosity calculation in CDF Note 6711.
- We made nearly identical selection requirements on our Z signal. The exceptions affected a negligible number of events. The exceptions were the track χ^2 cut, the CMU fiducial cuts (when reproducing the result we cut at 0.0 on the CMU X and Z fiducial distances), and the cosmic cut. See CDF note 6711 for the old cuts and Section 5 of this note for the new cuts.

The results of the comparison are shown in Tables 15 and 16. The old results are from CDF Note 6711, page 92, equations 49 to 52, after dividing by 1.004 to convert to the Z/γ^* cross section from the Z cross section. Note that both the old and new cross sections compared in this section do not have the NNLO acceptance correction.

We did not expect to be able to exactly reproduce the results from the published analysis. We used data reconstructed with a 5.3.1 release. The data used in the 72 pb^{-1} results were reconstructed using a 4.11.1 release. We used a new simulation sample generated with a modified 5.3.3 release. In the next few paragraphs we discuss these differences and expected statistical fluctuations resulting from them. In the end, our conclusion will be that the results are consistent considering these expected statistical fluctuations.

	Old	New CMX Bad	New CMX Good	New
CMUP/CMX + Track				
N_Z	1785	317	1467	1784
A_Z	0.1387	0.1115 ± 0.0012	0.1461 ± 0.0008	0.1384
A_Z CMX Good	0.1464			
ϵ_{tot}	0.713	0.731	0.726	0.727
$\int \mathcal{L}dt$	72.0	16.0 - 0.094	56.0 - 0.259	71.647
$\sigma \cdot B(Z/\gamma^* \to \mu\mu)$	248.9 ± 5.9	243.0 ± 13.8	246.7 ± 6.5	246.0 ± 5.9
CMUP + Track				
N_Z	1371	317	1052	1369
A_Z	0.1130	0.1115 ± 0.0012	0.1122 ± 0.0007	0.1120
ϵ_{tot}	0.663	0.731	0.658	0.674
$\int \mathcal{L}dt$	72.0	16.0 - 0.094	56.0 - 0.259	71.647
$\sigma \cdot B(Z/\gamma^* \to \mu\mu)$	252.1 ± 6.8	242.6 ± 13.7	253.6 ± 7.9	250.9 ± 6.8
CMX + Track				
N_Z	677		683	
A_Z	0.0603		0.0610 ± 0.0005	
ϵ_{tot}	0.796		0.814	
$\int \mathcal{L}dt$	55.5		55.5 - 0.259	
$\sigma \cdot B(Z/\gamma^* \to \mu\mu)$	252.2 ± 9.7		246.9 ± 9.5	

Table 16: Details of comparison between new and old cross section calculation. "Old" refers to the cross section calculation documented in CDF note 6711. "CMX Bad" refers to runs from 141544 to 149685. "CMX Good" refers to runs from 150799 to 156487. The last column refers to runs in both ranges together. N_Z is the number of Z candidates. A_Z is the acceptance measured from the simulation. ϵ_{tot} is the total efficiency. A background of 0.0075% is assumed in these calculations. Statistical errors on the acceptance are shown. All other errors are strongly correlated because we are comparing the same data. The last column is generated from the previous two columns: N_Z and $\int \mathcal{L}dt$ are the sum, A_Z and ϵ_{tot} are luminosity weighted averages, and the cross sections are averages weighted by the statistical errors, which are shown. We show data with CMX bad only for this comparison. It is not used in the new analysis.

1. We used a new simulation sample. Statistically our new acceptance is independent of the old. When one compares acceptances in Table 16, they are consistent within statistical uncertainty. Roughly, the fractional uncertainty on the acceptance is about 0.6% in the "CMUP/CMX + Track" and the "CMUP + Track" channel, the fractional uncertainty on the difference is roughly 0.9%. The uncertainty on the difference in $\sigma \cdot B$ between our new analysis and the old should be roughly 2.2 pb. In the "CMX + Track" channel, the uncertainty is a little higher, roughly 2.9 pb.

2. When one compares the list of events in the old and new Z candidate samples one finds that a surprising number of candidates were lost and added. Victoria Martin first noticed this (see page 21 of CDF Note 7031 [15]). We find that out the 1785 Z candidates, 53 were lost and 52 added. Most of this is due to the new reconstruction code in release 5.3.1. From simple Poisson statistics on the signal, one could expect $\sqrt{53 + 52}/1785 = 0.6\%$ fluctuations on the signal. This corresponds to an uncertainty on the $\sigma \cdot B$ difference of roughly 1.5 pb. In the "CMUP + Track" sample the uncertainty is roughly 0.7% or 1.8 pb. In the "CMX + Track" sample the uncertainty is roughly 0.9% or 2.3 pb.

3. The largest expected uncertainty on the difference in $\sigma \cdot B$ is also the most complicated and difficult to understand. It is related to the efficiencies. It is most significant for the track and isolation ID efficiencies, so we will focus on those. If one examines the 53 events that are lost going to release 5.3.1, one finds that 33 of the 53 were lost due to the track ID and isolation cuts (14 segment cut + 8 hadron energy cut + 5 isolation cut + 5 impact parameter cut + 1 χ^2 cut). We did not examine this, but it is reasonable to assume that a similar number of candidates were added due to the same cuts. Based on the efficiencies from CDF Note 6711, we expect the total number of candidates removed by the track ID and isolation cuts is roughly 289. The fraction coming in and out of this subset of events is surprisingly large, roughly 33 · 2 / 289 or 23%. This can cause significant statistical fluctuations in the measured values of these efficiencies. One cannot expect the efficiencies to have identical values simply because we use the same good run list. We expect systematic shifts and statistical fluctuations. The uncertainty on the difference in $\sigma \cdot B$ should be roughly equal to $\sqrt{0.23}$ times the total statistical uncertainty on the $\sigma \cdot B$ due to these efficiencies. Using the efficiencies from CDF Note 6711 and remembering that we must square them, the total efficiency of the Z selection due to isolation and track ID cuts is 0.8382 $\pm$ 0.0128 in the "CMUP/CMX + Track" case. Translating to an uncertainty on $\sigma \cdot B$, the uncertainty is 3.8 pb. The *statistical* uncertainty on the difference between the 4.11.1 and 5.3.1 efficiency is $\sqrt{0.23} \cdot 3.8 = 1.8$ pb. In addition there could also be systematic shifts, but these would cancel out in the $\sigma \cdot B$ calculation. Now we repeat this for the other two channels. For "CMUP + Track", the total isolation and track ID efficiency is 0.8291 $\pm$ 0.0157. The uncertainty on $\sigma \cdot B$ is 3.9 pb. The uncertainty on the difference is roughly 2.0 pb. For "CMX + Track", the total isolation plus track efficiency is 0.8667 $\pm$ 0.0215. The uncertainty on $\sigma \cdot B$ is 6.2 pb. The uncertainty on the difference in $\sigma \cdot B$ is roughly 3.0 pb.

Adding in quadrature the uncertainty from the 3 sources discussed above yields the following level of expected deviations between $\sigma \cdot B$ using release 4.11.1 and 5.3.1. For the "CMUP/CMX + Track" case, it is 3.2 pb. For the "CMUP + Track" case, it is 3.5 pb, and for the "CMX + Track" case, it is 4.8 pb.

A.1 Step 1 - Remove Luminosity Error

	CMUP/CMX + Track (pb)	CMUP + Track (pb)	CMX + Track (pb)
With error	246.0 ± 5.9	250.9 ± 6.8	246.9 ± 9.5
Without error	245.6 ± 5.9	250.9 ± 6.8	244.7 ± 9.4

Table 17: $\sigma \cdot B$ with statistical uncertainty with and without the luminosity error. Differences are small.

In the 72 pb^{-1} cross section measurement documented in CDF Note 6711, there was a small error in the luminosity. The error was that 55.5 pb^{-1} was used as the luminosity with the CMX detector good. The correct value was 56.0 pb^{-1}. The total luminosity was correct at 72.0 pb^{-1}, only the split between the good and bad CMX luminosities was incorrect. We intentionally reproduced that error above. Its effect was largest in the "CMX + Track" measurement where it was simply a luminosity error. In the "CMUP/CMX + Track" channel, the error had a small effect when averaging the acceptances for the data with CMX good and bad. We believe it did not affect the efficiency, although it is possible there was also some small effect there we have not accounted for. Table 17 shows the difference in the $\sigma \cdot B$ related to this error.

A.2 Step 2 - Use New Good Run Lists

	CMUP/CMX + Track (pb)	CMUP + Track (pb)	CMX + Track (pb)
WZCS_2003	245.6 ± 5.9	250.9 ± 6.8	244.7 ± 9.4
WZCS_2003_2	246.3 ± 6.5	253.6 ± 7.9	244.7 ± 9.4
DQM 4.0		255.2 ± 4.3	
muon_nosi_1	248.8 ± 6.1	257.3 ± 7.4	243.7 ± 8.8
muon_nosi_2	254.6 ± 4.5	256.1 ± 5.4	248.9 ± 6.7
muon_nosi_3	249.4 ± 7.2	251.2 ± 8.5	245.4 ± 10.7
muon_nosi_4	256.8 ± 5.0	260.4 ± 5.9	244.1 ± 7.3
muon_nosi	253.3 ± 2.7	256.7 ± 3.3	245.9 ± 4.0

Table 18: $\sigma \cdot B$ with statistical uncertainty using different run lists from different time periods. The run lists are defined in the text.

Next we changed to the standard DQM 7.0 good run lists. We used the "muon no silicon" list that requires the CMUP and CMX both be good for all runs, with no electron or silicon requirements. We divided the runs into the following ranges to study the time dependence. The $\sigma \cdot B$ for the old and new run lists are shown in Table 18.

- WZCS_2003 is the old run list from run 141544 to 156487. It was used in CDF Note 6711. This is the 72.0 pb^{-1} dataset.

- WZCS_2003_2 is the old run list from run 150799 to 156487 with CMUP and CMX good.

- DQM 4.0 is the run list that was used for the results in Alexei Varganov's thesis [16]. It contains runs from March 2002 to September 2003, 141544 to 168889.

- muon_nosi is all runs on the DQM 7.0 muon no silicon good run list before the August 2004 shutdown.

- muon_nosi_1 is the subset of muon_nosi before the January 2003 shutdown. It has a large overlap with WZCS_2003_2. It includes runs from 150145 to 156487.

- muon_nosi_2 is the subset of muon_nosi between the January 2003 shutdown and the September 2003 shutdown. It includes runs from 158644 to 168889.

- muon_nosi_3 is the subset of muon_nosi between the September 2003 shutdown and the start of the COT compromised period. It includes runs from 174997 to 179056.

- muon_nosi_4 is the subset of muon_nosi between the end of the COT compromised period and the August 2004 shutdown. It includes runs from 182843 to 186598.

Alexei Varganov's thesis [16] reported $\sigma \cdot B(Z/\gamma^* \to \mu\mu)$ for a 193.5 pb^{-1} DQM 4.0 dataset using only CMUP trigger muons. His result was 252.1 pb. Table 18 shows that we get 255.2 pb for this data sample using the version of our code that reproduces the 72 pb^{-1} result. There are several differences in Alexei's analysis, some that we identified and studied and possibly some others we missed. Only two of the differences we studied caused a shift in $\sigma \cdot B$ larger than 1 pb. When calculating the acceptance, Alexei used the HEPG muons after final state radiation to count generated Z's used in the acceptance denominator. Fewer generated Z's fall in the 66 to 116 GeV mass window which raises the acceptance and lowers the cross section. This is not the standard way of doing the calculation, and it is not what was done in the 72 pb^{-1} analysis, where they counted using the muons before final state radiation. Usually people count before to make the comparison with theorists predictions easier, because that is how theorists calculate their results. When we use the muons after final state radiation to attempt to reproduce Alexei's result, we find the $\sigma \cdot B$ goes from 255.2 pb to 248.8 pb, a 2.6% shift. Alexei's background estimate is 0.36% compared to the 0.75% value in CDF Note 6711. When we also use Alexei's background estimate we find $\sigma \cdot B$ goes from 248.8 pb to 249.8 pb. We are 2.3 pb or 0.9% lower than Alexei's result of 252.1 pb. In 72 pb^{-1}, we expected the uncertainty on the difference to be roughly 3.5 pb. If we scale this uncertainty by the square root of the luminosity difference the uncertainty on the difference for this data set is 3.5 x $\sqrt{72.0/193.5} = 2.1$ pb. The difference between our result and Alexei's result is consistent with this uncertainty. We have successfully reproduced Alexei's result within the expected uncertainties.

Efficiency Application	CMUP/CMX + Track (pb)	CMUP + Track (pb)	CMX + Track (pb)
Old	253.3 ± 2.7	256.7 ± 3.3	245.9 ± 4.0
Only Data Eff	252.9 ± 2.7	254.5 ± 3.2	249.8 ± 4.1
Scale Factor	257.7 ± 2.8	259.7 ± 3.3	254.5 ± 4.1

Table 19: $\sigma \cdot B$ with statistical uncertainty using different methods to apply the individual efficiencies to the data. Described in more detail in the text.

A.3 Step 3 - Method of Using Efficiencies

Efficiencies are calculated for different cuts or sets of cuts. There are a variety of ways one can use these efficiencies to calculate an overall efficiency to apply to the signal count to get the cross section. One must choose to either:

- Model the efficiency cut exclusively with an efficiency derived from data. In this case, one must also not make a cut when deriving the acceptance from the simulation and not use the efficiency for the cut derived from simulation.
- Or make the cut when deriving the acceptance from simulation. Use both the efficiency calculated from data and from simulation to calculate a scale factor to account for discrepancies between the simulation and data efficiencies.

Given infinite statistics, one could imagine getting the same result using either of the above methods. In addition to this choice, one also needs to decide how to divide the data sample to apply different efficiencies. Some approximations are necessary in this process. Table 19 shows results using three different choices of ways to use the efficiencies.

- The row labeled "Old" is a calculation where we have attempted as best we can to recreate the calculation used for the previously published result. The details are lengthy and not repeated in this note, but they are presented in CDF Note 6711. Some of the highlights are as follows. The data is divided into two subsets: candidates where one leg hits a muon detector and candidates where two legs hit a muon detector. Stub related efficiencies are applied based on the fraction of Z candidate that falls in each subset. For the "CMUP + Track" channel, efficiencies measured with the test track pointing at CMUP are used. For the "CMX + Track" channel, efficiencies measured with the test track pointing at CMX are used. For the "CMUP/CMX + Track" channel, efficiencies measured with CMUP and CMX test legs are averaged (which is only approximately correct). The data only efficiencies are used for the d_0, EM, HAD, isolation, track χ^2, DX, and segment cuts. A scale factor is used for the muon reconstruction efficiency, although there is an approximation in the calculation because the scale factor is algebraically applied like it was a data only efficiency.
- The row labeled "Only Data Eff" is different in several ways. The data are divided into seven subsamples, CMUP + CMUP, CMUP + CMX, CMX + CMX, CMUP + Track, and CMX + Track, where the track can either be in the CMUP or CMX detector η region. Stub and track Efficiencies are applied based on whether the muon or track is

in the detector η region of the CMUP or CMX. The formulas used to do this are more exact than in the old method. The muon reconstruction efficiency is properly treated as a scale factor and the other ID efficiencies are treated as data only efficiencies.

- The row labeled "Scale Factor" is similar to the previous case except all the efficiencies other than the trigger efficiency are treated as scale factors. This is the method used for the new analysis and it is discussed extensively in the efficiency section of this note.

In Table 19, the methods agree within 2%. The disagreements are large enough to require some explanation. The dominant reason the "Old" and "Only Data Eff" rows differ is related to the fact that in the old method in the "CMUP + Track" case, efficiencies measured using CMUP test legs are used for all muons and tracks. The "Track ID with isolation" efficiency measured using CMUP test legs differs from the same efficiency measured using CMX test legs by about 2%. Using this efficiency for legs pointing towards CMX detector η creates a bias upward on $\sigma \cdot B$. A similar problem exists in the "CMX + Track" sample and moves $\sigma \cdot B$ a larger amount in the opposite direction. The problem is smaller in the "CMUP/CMX + Track" sample, but here the averaging of efficiencies is only approximately correct. Note that the difference in the "Track ID with isolation" efficiencies measured with CMUP and CMX is created mostly by the COT segment cut which we will later loosen. The differences between the "Only Data Eff" results and the "Scale Factor" results are related to a bias created by a mass window cut in the acceptance calculation. We discuss changing this in the next section.

A.4 Step 4 - Remove Tight Mass Cut in ID Efficiency Calculation

Efficiency Application	CMUP/CMX + Track (pb)	CMUP + Track (pb)	CMX + Track (pb)
With 80 to 100 GeV Mass Requirement in ID Efficiency Calculation			
Old	253.3 ± 2.7	256.7 ± 3.3	245.9 ± 4.0
Only Data Eff	252.9 ± 2.7	254.5 ± 3.2	249.8 ± 4.1
Scale Factor	257.7 ± 2.8	259.7 ± 3.3	254.5 ± 4.1
Without 80 to 100 GeV Mass Requirement in ID Efficiency Calculation			
Old	259.8 ± 2.8	263.8 ± 3.3	251.6 ± 4.1
Only Data Eff	259.4 ± 2.8	261.4 ± 3.3	255.9 ± 4.2
Scale Factor	258.5 ± 2.8	260.7 ± 3.3	254.9 ± 4.2

Table 20: $\sigma \cdot B$ with statistical uncertainty before and after changing the Z mass requirement on the sample used to calculate the ID efficiencies.

The ID efficiencies are significantly lower in the sample of Z candidates with mass between 66 GeV and 80 GeV than between 80 GeV and 100 GeV. In the lower mass region, there is a significant fraction of candidates that underwent bremsstrahlung or final state radiation. That is why they have a lower mass. For the same reason, there is more nearby radiation and these candidates tend to fail the EM energy and isolation cuts more often. This causes their ID efficiency to be lower. If one measures ID efficiencies in the 80 to 100 GeV mass sample and then uses the 66 to 116 GeV sample as signal, there is a bias. In the 72 pb^{-1} analysis which we have been reproducing, the efficiencies were measured with a sample with the mass between 80 and 100 GeV. We remove the bias by using a 66 to 116 GeV cut when calculating the efficiencies. The results of this change are shown in Table 20.

In the past, people have used the tight mass cut to remove background, but the bias it creates is a larger problem than the background. The bias it creates is on the order of 1%, which gets doubled when applied to the Z cross section because it affects both legs.

In Table 20 one can see that the "Only Data Eff" result rises and becomes nearly equal to the "Scale Factor" result when this bias is removed. This is because the simulation corrects for the bias in the scale factor method.

A.5 Step 5 - Loosen COT Segment Cut

Efficiency Application	CMUP/CMX + Track (pb)	CMUP + Track (pb)	CMX + Track (pb)
With Tight COT Segment Cut			
Old	259.8 ± 2.8	263.8 ± 3.3	251.6 ± 4.1
Only Data Eff	259.4 ± 2.8	261.4 ± 3.3	255.9 ± 4.2
Scale Factor	258.5 ± 2.8	260.7 ± 3.3	254.9 ± 4.2
With Loose COT Segment Cut			
Old	261.4 ± 2.7	264.6 ± 3.2	254.8 ± 4.0
Only Data Eff	261.1 ± 2.7	263.3 ± 3.2	257.1 ± 4.0
Scale Factor	260.3 ± 2.7	262.7 ± 3.2	256.3 ± 4.0

Table 21: $\sigma \cdot B$ with statistical uncertainty before and after loosening the COT segment cut.

We loosen the COT segment cut. In the published 72 pb^{-1} analysis, the requirement was 3 axial and 3 stereo segments with 7 hits per segment. We require 3 axial and 2 stereo segments with 5 hits per segment. These are the new loose track quality cuts recommended by the tracking group. The tight cut is not needed to reject background and this increases the number of Z candidates. There are also pathologies associated with measuring the efficiency of a tight segment cut that we avoid. The tight cut is not homogeneous geometrically. More tracks fail it at low $|\eta|$, more fail in CMUP than in CMX, and also there there is a spike in the ϕ distribution of the ones that fail near $\phi = 0$ radians. Because the geometry is not exactly the same in the sample of test legs as in the sample of legs of Z candidates, it is plausible this might introduce a bias in the efficiency. Also the rate of tracks failing the cut is luminosity dependent. More interactions in a crossing makes the tracks more likely to fail the segment cut. This introduces a correlation between the probability that the two legs of a Z candidate will pass the segment cut. Table 21 shows $\sigma \cdot B$ before and after we loosen the segment cut. Although there are reasons to worry about biases, the difference in $\sigma \cdot B$ is small. We estimated the statistical uncertainties involved and the difference is only roughly 1.5 standard deviations. It could just be a statistical fluctuation.

We use a very loose segment cut to avoid these issues and complications. Since our segment requirement is near 100% efficient, there can be no bias.

Efficiency Application	CMUP/CMX + Track (pb)	CMUP + Track (pb)	CMX + Track (pb)
With Loose COT Segment Cut			
Old	261.4 ± 2.7	264.6 ± 3.2	254.8 ± 4.0
Only Data Eff	261.1 ± 2.7	263.3 ± 3.2	257.1 ± 4.0
Scale Factor	260.3 ± 2.7	262.7 ± 3.2	256.3 ± 4.0
With Loose CMU DX Cut			
Old	261.7 ± 2.7	265.0 ± 3.2	254.9 ± 4.0
Only Data Eff	261.5 ± 2.7	263.6 ± 3.2	257.3 ± 4.0
Scale Factor	260.7 ± 2.7	263.1 ± 3.2	256.4 ± 4.0
With Modified z_0, d_0, and Muon Fiducial Cuts			
Old	261.6 ± 2.7	265.4 ± 3.2	254.4 ± 4.0
Only Data Eff	261.5 ± 2.7	264.1 ± 3.2	256.5 ± 4.0
Scale Factor	260.5 ± 2.7	263.5 ± 3.2	255.5 ± 4.0
Tighter Selections to Measure ID Efficiencies			
Old	260.6 ± 2.7	264.2 ± 3.2	253.6 ± 4.0
Only Data Eff	260.4 ± 2.7	263.0 ± 3.2	255.6 ± 4.0
Scale Factor	259.5 ± 2.7	262.4 ± 3.2	254.7 ± 4.0
Set Cosmic Background Estimate to 0			
Old	262.3 ± 2.7	265.9 ± 3.2	255.3 ± 4.0
Only Data Eff	262.2 ± 2.7	264.8 ± 3.2	257.3 ± 4.0
Scale Factor	261.2 ± 2.7	264.1 ± 3.2	256.4 ± 4.0

Table 22: $\sigma \cdot B$ with statistical uncertainty as cuts are modified.

A.6 Step 6 - Loosen CMU DX Cut

Loosening the CMU DX cut from 3 cm to 7 cm significantly increases the efficiency of the cut. The events that are recovered are good Z bosons without any indications of any significant background. As can be seen from Table 22, the result for $\sigma \cdot B$ does not change significantly when this cut is changed.

A.7 Step 7 - Modify d_0, z_0, and Muon Fiducial cuts

The changes to the d_0, z_0, and Muon Fiducial cuts used to select Z signal candidates do not have a large effect on $\sigma \cdot B$. The effect of these modifications is shown in Table 22. This is not a surprise because only a small number of candidates are affected by these changes. The changes are motivated more on principal than on their significance to the final result. Along with this we also modified the z_0 cut made in the ID efficiency sample to be the same as the cut used in the Z selection.

A.8 Step 8 - Tighter Selections to Measure ID Efficiencies

There are conflicting goals when establishing the cuts on the first trigger leg in the ID efficiency measurement. On the one hand, one wants the cuts to be tight to remove background. On the other hand, one worries that the two legs are correlated and that cuts on the first leg will bias the efficiency measurement on the second. One wants to minimize background, but remove as few test legs as possible to minimize any bias due to correlations.

Detector	Opposite Sign	Same Sign
Method from Published 72 pb^{-1} Analysis		
CMUP	5413	6
CMX	2845	3
Wider Mass Window		
CMUP	6011	13
CMX	3107	9
Muon Fiducial and z0 Change		
CMUP	6022	13
CMX	3113	9
Option 1: Add Full Muon ID Cuts on First Leg		
CMUP	5508	4
CMX	2793	3
Option 2: Add Loose Isolation, d_0, and Tighter CMX DX cuts		
CMUP	5989	7
CMX	3091	4

Table 23: Number of test legs in sample used to measure ID efficiencies as cuts to select the sample of test legs are modified. The number of same sign events gives an estimate of the background in the opposite sign sample.

We started with the selections used for the published 72 pb^{-1} measurement. As described 3 sections ago, we widened the Z mass window from 80:100 GeV to 66:116 GeV, which increased the amount of background. The bias due to this additional background is significantly smaller than the bias created by the narrow mass window. As described in the previous section, we made changes to the z_0 and muon fiducial requirements that affect the ID efficiencies in a negligible way. Table 23 shows the number of test legs we have in the ID efficiency sample for different selections. It also shows the number of test legs passing similar cuts, except with the same sign charge instead of opposite sign. One can use the number of same sign test legs as an estimate of the background in the sample we are using to measure the ID efficiencies. There are also a small number of cosmics in the sample. We measured the cosmic background in the ID efficiency sample using the same method as used to measure the cosmics in the signal sample.

More recent ID efficiency measurements have made a full set of muon identification cuts on the first leg, which are much tighter. See for example CDF Notes 7367 [7] and 7031 [15]. Table 23 shows the effect of making the full set of muon identification cuts on the first leg in this analysis. The background is reduced, but a substantial number of test legs are also lost.

After trying many possibilities, we find that adding only three new requirements to the first leg instead of making the full set of muon ID cuts on the first leg greatly reduces the background without removing many test legs. These three additional selections are

1. Require the first leg pass a loose isolation cut, isolation / $p_T < 0.4$. This reduces QCD background.

2. Require the first leg pass a d_0 cut, $|d_0| < 0.4$ cm. This gets rid of a few cosmics.

3. Require the first leg pass a $|dx| < 6.0$ cm cut if it is a CMX leg, just because the old 20 cm cutoff is ridiculously large.

Table 23 also shows the number of test legs and same sign legs passing these requirements. It removes almost as many same sign legs as using the full set of muon ID cuts, but removes many less opposite sign test legs. These are the cuts we use to measure the efficiency. Table 22 shows the effect on $\sigma \cdot B$ of using these cuts to measure the ID efficiencies. Because more background is removed, the efficiencies rise and the $\sigma \cdot B$ falls by a small amount.

The remaining QCD background in the ID efficiency sample is about a part in a thousand (based on the number of same sign test legs). Our upper limit on the cosmic contamination is about at the same level. The systematic errors caused by this are significantly smaller than the statistical errors on the efficiency, so we simply ignore them. In a future analysis with 10 times more data, these errors will no longer be small compared to the statistical uncertainty on the ID efficiencies and will need to be estimated.

A.9 Step 9 - Set Cosmic Background Estimate to 0

As described in Section 6.2, we estimate the cosmic background in the Z signal at 0. This is compared to a previous estimate of 13.3 cosmics in 1785 Z signal events. Table 23 shows the effect on $\sigma \cdot B$ of lowering the background estimate from 0.0075 to 1.5 / 1785 = 0.00084, which is the $Z \rightarrow \tau\tau$ rate from CDF Note 6711. As expected, $\sigma \cdot B$ rises a small amount because we subtract a smaller background estimate from the signal.

A.10 Summary, $\sigma \cdot B$ for Each Change

Table 24 shows the variation in $\sigma \cdot B$ for each step described above.

A.11 Cross Check $\sigma \cdot B$ in Different Run Ranges

With this final analysis method we calculate the $\sigma \cdot B$ again in the four run ranges described earlier in Section A.2. The results are shown in Table 25. Variations are consistent with statistical fluctuations. We see no evidence of systematic shifts in $\sigma \cdot B$ with time.

Modification	Change in $\sigma \cdot B$ (pb)
Published 72 pb^{-1} Result	Starting Point
Reproduce 72 pb^{-1} Result***	-2.9
Luminosity Fix	-0.4
Run List***	+7.7
ID Efficiency Mass Window	+6.5
Efficiency Algorithms***	-1.3
Segment Cut (?)	+1.8
CMU DX Cut***	+0.4
z_0, d_0, and Muon Fiducial***	-0.2
ID Efficiency Selections	-1.0
Cosmic Background	+1.7

Table 24: Change in $\sigma \cdot B$ with each modification in the analysis. This is for the "CMUP/CMX + Track" channel. The rows labeled with a "***" are consistent with statistical fluctuations and we can think of no reason they would cause a systematic shift. We are not sure about the segment cut. It is likely a systematic shift, but possibly statistical. The others are systematics shifts whose cause is understood.

	CMUP/CMX + Track (pb)	CMUP + Track (pb)	CMX + Track (pb)
muon_nosi_1	257.7 ± 6.1	262.7 ± 7.2	259.1 ± 9.1
muon_nosi_2	264.7 ± 4.5	268.9 ± 5.4	257.1 ± 6.7
muon_nosi_3	252.0 ± 6.9	251.4 ± 8.0	251.9 ± 10.5
muon_nosi_4	264.4 ± 4.8	266.8 ± 5.7	256.0 ± 7.3
muon_nosi	261.2 ± 2.7	264.1 ± 3.2	256.4 ± 4.0

Table 25: $\sigma \cdot B$ with statistical uncertainty for different run lists from different time periods. The run lists are defined in the text. We show only the results using the scale factor efficiency method here.

References

[1] D. Amidei *et al.*, CDF Note 6711, 3 Mar 2004 (unpublished).

[2] D. Acosta *et al.*, Phys. Rev. Lett. **94**, 091803 (2005).

[3] A. Abulencia *et al.*, arXiv:hep-ex/0508029 12 August 2005 (submitted to PRD).

[4] S. Jindariani *et al.*, CDF Note 7446, 31 Jan 2005 (unpublished).

[5] C. Hays (private communication).

[6] L. Nodulman, CDF Note 6971, 1 Oct 2004 (unpublished).

[7] V. Martin, CDF Note 7367, 19 Nov 2004 (unpublished).

[8] J. Bellinger *et al.*, CDF Note 5870, 4 Nov 2002 (unpublished).

[9] H. Gerberich *et al.*, CDF Note 6089, 29 Aug 2002 (unpublished).

[10] S. Waschke, CDF Note 6088, 28 Jan 2003 (unpublished).

[11] S. Cabrera *et al.*, CDF Note 6909, 21 Sept 2004 (unpublished).

[12] T. Sjöstrand *et al.*, Computer Physics Commun. **135**, 238 (2001).

[13] W. K. Sakumoto, CDF Note 7324, 28 Oct 2004 (unpublished).

[14] D. Glenzinski *et al.*, CDF Note 5973, 25 Feb 2003 (unpublished).

[15] V. Martin, CDF Note 7031, 2 Nov 2004 (unpublished).

[16] A. Varganov, Ph.D. thesis, University of Michigan, 2004 (also CDF Note 7163).